Author Manuscript

Title: Nitric Oxide Release for Enhanced Biocompatibility and Analytical Performance of Implantable Electrochemical Sensors

Authors: Qi Zhang, Mark Meyerhoff

This is the author manuscript accepted for publication. It has not been through the copyediting, typesetting, pagination and proofreading process, which may lead to differences between this version and the Version of Record.

To be cited as: 10.1002/elan.202100174

Link to VoR: https://doi.org/10.1002/elan.202100174

Nitric Oxide Release for Enhanced Biocompatibility and Analytical Performance of Implantable Electrochemical Sensors

Qi Zhang [a], Mark E. Meyerhoff [a] *

[a] Department of Chemistry, University of Michigan, Ann Arbor, MI 48109, USA

* Corresponding author

email: mmeyerho@umich.edu

Author Manuscript

*This article is dedicated to the memory of Jean-Michel Saveant

This article is protected by copyright. All rights reserved

ABSTRACT

The real-time, continuous monitoring of glucose/lactate, blood gases and electrolytes by implantable electrochemical sensors holds significant value for critically ill and diabetic patients. However, the wide-spread use of such devices has been seriously hampered by implant-initiated host responses (e.g., thrombus formation, inflammatory responses and bacterial infection) when sensors are implanted in blood or tissue. As a result, the accuracy and usable lifetime of *in vivo* sensors are often compromised. Nitric oxide (NO) is an endogenous gas molecule able to inhibit platelet adhesion/activation, inflammatory responses and bacterial growth. As such, the release of NO from the surfaces of *in vivo* sensors is a promising strategy for enhancement of their biocompatibility and analytical performance. In this review, the physiological functions of NO to improve the biocompatibility of implantable electrochemical sensors are introduced, followed by a brief analysis of chemical approaches to realize NO release from such devices. A detailed summary of the various types of NO releasing electrochemical sensors reported to date and their performance in benchtop and/or *in vivo* testing are also provided. Finally, the prospects of future developments to further advance NO releasing sensor technology for clinical use are discussed.

Author Manuscript

1. Introduction

Frequent and accurate measurements of critical care analytes, such as glucose/lactate, blood gases (pH, PO_2, PCO_2) and electrolytes (Na^+, K^+, Ca^{2+}) in undiluted circulating whole blood hold great value for patients in intensive care units and operating rooms. Currently, the clinical standard of care largely relies on intermittent *in vitro* blood tests on benchtop instruments or point-of-care devices. The delayed diagnosis/therapeutics and a high risk of infection can be life-threatening to the critically ill patients. Therefore, the development of implantable devices that continuously monitor clinically important species can lead to much improved outcomes for such patients [1-6]. Moreover, tight control of glucose concentrations via *in vivo* monitoring of glucose in blood or the interstitial fluid could significantly enhance the quality of life for millions of non-hospitalized patients with diabetes mellitus [7-8].

Over the past decades, real-time monitoring of critical care species via implanted sensors in blood vessels (intravascularly) or under the skin within subcutaneous fluid (subcutaneously) has been pursued for improved patient care. Major criteria for such implantable chemical sensors include: (1) sufficiently miniaturized to be implanted; (2) provide long-term stable analytical signals that accurately follow the concentration of a given analyte and (3) be biocompatible with the host environment in which the sensor is implanted. Significant

This article is protected by copyright. All rights reserved

progress has been achieved in engineering miniaturized chemical sensing devices in the recent years. However, despite extensive research efforts, designing successful implantable sensors that yield accurate enough results for continuous *in vivo* use is still complicated by adverse biological responses of living systems toward the miniaturized sensors as foreign bodies/materials, commonly referred to as the biocompatibility problem [9-11]. The aberrant biocompatibility between the host environment and the surface of the sensor elicits thrombus formation and/or inflammatory responses, primarily depending on the location of implantation: blood or subcutaneous tissue. These pathological host responses to implantable devices create a multi-factorial barrier to successful application of implantable biosensors and addressing these issues represents an unmet need in the field of critical care monitoring.

Intravascular chemical sensors offer the potential to provide direct and almost instantaneous assessment of a given analyte concentration in a patient's blood and is, therefore, of enormous diagnostic/therapeutic value. However, such value is thwarted by thrombosis concerns and erratic *in vivo* accuracy resulting from the hostile and complex analytical environment (blood). Indeed, to date, no intravascular chemical sensor has been approved to be used in humans for continuous monitoring. The thrombus formation processes associated with blood-contacting sensors [12-14] is illustrated in Fig. 1(a). Upon implantation, proteins (e.g., fibrinogen, von Willebrand's factor, fibronectin and vitronectin) will nearly instantaneously adsorb on the blood-contacting sensor surface, which then present anchoring sites for platelets to adhere. Platelet adhesion and subsequent activation rapidly trigger a coagulation cascade, converting soluble fibrinogen to insoluble fibrin and eventually leading to clot formation on the surface of the device. With the presence of this thrombus layer, the concentration of analytes within microenvironment around the sensor's surface no longer represents their actual levels in bulk blood [13, 15-16]. Indeed, the adherent metabolically active cells will consume O_2 and glucose and produce CO_2, which will lower pH due to the elevated CO_2 level (Fig. 1(b)). The mass transport of analytes species from bulk blood to the sensor surface is also impacted due to blockage by the thrombus layer as well as reduced blood flow due to vasoconstriction of the artery or vein. Even worse, thrombus formation is a largely random process in patients as the activation and adhesion of platelets depend on various factors, including the blood flow in the lumen where the sensor is implanted, the size (diameter) of the blood vessel, and the intrinsic coagulation propensity of a given patient

Also, when the sensor touches the inner wall of a blood vessel, the inherent metabolism of endothelial cells that line the vessel can affect the sensor reading in the same way as adhered platelets (also known as "wall effect") [12, 17-18]. In addition, the adhesion of bacteria and biofilm formation at the intravascular sensor surface could lead to bacterial infection, a serious complication [19]. Intravascular sensor performance is,

This article is protected by copyright. All rights reserved

Author Manuscript

therefore, often unreliable and unpredictable due to these biological factors, preventing timely therapeutic intervention.

Subcutaneous/percutaneous chemical sensors, in particular indwelling amperometric continuous glucose monitors (CGMs) for diabetic patients, have gained significant commercial success in the past decade [8, 20-22]. This is because tissue concentrations for glucose correlate well with their levels in blood, while the correlation is often fairly poor for other analytes [23, 24]. However, continuous improvement of sensor biocompatibility, through tackling the foreign body response (FBR), remains a crucial step to achieve shorter lag time and longer usable lifetime in the next generation of subcutaneous glucose sensors [12, 25-27]. FBR is a cascade of intense inflammatory/wound healing reactions that transpire at the surface of the implanted device. After sensor implantation in subcutaneous tissues, acute inflammatory response rapidly takes place once fluids and plasma proteins migrate to the implant site and adhere to the sensor surface, followed by the influx of neutrophils, monocytes and macrophages onto the implanted device to initialize the process of phagocytosis [28]. After the acute inflammatory response (24 – 48 h), a fibrous capsule, primarily by macrophages and collagen, forms around the implanted sensor. This capsule can change local analyte levels through metabolic activities (e.g., accelerated glucose consumption). Further, the foreign body capsule forms a barrier that significant alters the analyte diffusion to the sensor surface as well as its transfer between the blood vessels and the interstitial fluid, greatly influencing the response curve/sensitivity and lag time of the sensor [16, 27, 29-30]. Meanwhile, the output of subcutaneous sensors is also affected by the degree of angiogenesis around the site of tissue injury (as a wound-healing process) caused by sensor implantation [31-32]. That is, limited new blood vessel formation near the subcutaneous sensor could lead to a low flux of analyte into the subcutaneous fluid region adjacent to the sensor, causing poor reflection of analyte levels in the bloodstream, and vice versa. Once the chronic inflammatory response has stabilized, the effect of the capsule formation is partially responsible for the need of periodic finger-prick blood calibration, which was, until recently, considered a major drawback in many CGM systems [20-22, 33]. Some of the very latest subcutaneous electrochemical glucose sensors that have been commercialized (e.g., DexCom) no longer require repeated calibration each day, possibly due to the use of surface coatings that decrease the inflammatory response. However, it is uncertain that FBR has completely been prevented for such commercial devices, since calibration algorithms may still be required to compensate signal drifts caused by FBR. Also, similar to intravascular sensors, subcutaneous sensors can incur implant-associated infection that commonly leads to premature removal of the sensor [19]. Therefore, further improvement of device biocompatibility remains crucial for the next generation of implantable subcutaneous sensors.

This article is protected by copyright. All rights reserved

Author Manuscript

Surface modification strategies reported to address biocompatibility issues of implanted devices have largely focused on chemical or physical modifications to the outermost blood/tissue-contacting membrane of the implantable sensors to mitigate the thrombus-formation and FBR. The benefits and limitations of these strategies have been highlighted in a number of reviews [12, 16, 34-40]. Some of the approaches include hydrogels and zwitterion polymers [41-43], biomimicry (e.g., the attachment of phospholipids to coating surfaces) [44, 45], flow-based systems (by flowing fluid over material-tissue surface) [46-48], Nafion polymer coatings [49, 50], surfactant-derived membranes [51, 52], diamond-like carbons [53, 54] , use of polyurethane (PU) and silicone elastomers [55, 56], naturally derived materials [57, 58], porous and nanopatterned coatings [52, 53, 59, 60], and immobilization of biological molecules (e.g., heparin and hyaluronic acid) [61, 62]. In addition, "active" coatings that release or generate anti-inflammatory or pro-angiogenic bioactive agents such as dexamethasone (DX) [63], vascular endothelial growth factor (VEGF) [64], and the dual DX/VEGF delivery [65] have emerged as favorable candidates for more biocompatible sensor design. However, despite extensive efforts, none of these methods have managed to completely address the biocompatibility problems for fabrication of clinically useful chemical sensors implanted intravascularly or subcutaneously for patients.

Continuous, localized delivery of nitric oxide (NO), an endogenous free-radical gas molecule, from sensor surfaces was first proposed in late 1990s as a promising alternative solution for mitigating the aggressive reactions of the body toward implantable chemical sensors [66]. Due to NO's innate thromboresistant, anti-inflammatory, anti-microbial, and pro-angiogenic properties [67-71], there has been considerable progress in implementing NO release in various types of sensors over the last two decades, yielding much improved device biocompatibility and *in vivo* analytical accuracy. In particular, NO releasing electrochemical sensors have drawn considerably attention due to their overall low cost, fast response, operational simplicity and robustness for *in vivo* applications. Though there have been several review articles published in this field [13, 72], the present review focuses on NO release concepts employed in designing implantable electrochemical sensors to date and the evaluation of sensor performance both *in vitro* and *in vivo*. This review also takes on a new perspective to introduce NO releasing electrochemical sensors by the types of targets/analytes, and provides a chronological outline (Table 1) of all relevant sensors reported. This systematical approach is expected to help readers better follow the progress in the field. Prospects for future development of such devices toward eventual clinical applications as well as an account of exciting new NO generating materials/methods that are promising for sensor fabrication are also provided in this review article.

This article is protected by copyright. All rights reserved

Author Manuscript

2. Nitric oxide (NO) release as a strategy to enhance implantable sensor biocompatibility

2.1 Nitric oxide physiological functions

Nitric oxide (NO) is a short-lived, diatomic free radical ubiquitously produced in the body. It is synthesized from L-arginine by the enzyme nitric oxide synthase (NOS) [73]. Widely recognized as an effective anti-platelet, anti-inflammatory and vasodilating agent, NO is also known to be antibacterial and pro-angiogenic [71, 74-75]. Hence, NO has received enormous interest from the biomedical research community over the last three decades.

Nitric oxide's function as a potent anti-thrombotic agent primarily involves inhibition of platelet activation and aggregation on the implant, owing to NO binding to the heme moiety of soluble guanylate cyclase and the subsequent stimulation in the production of intracellular cyclic guanosine monophosphate (cGMP) [67, 76-77]. Indeed, within blood vessels, the production of NO by the normal endothelial cells that line the inner walls of all vessels, is the reason clots do not normally form on the inner surface of healthy blood vessels. Vasoconstriction can also occur as a physiological phenomenon to restrict bleeding at the implant site. When NO diffuses into vascular smooth muscle cells, it stimulates cGMP production and therefore, lowers the Ca^{2+} levels in the smooth muscle cells. This leads to vascular relaxation and blood vessel dilation [78].

Nitric oxide also plays a crucial role in mediating inflammatory response. While prior research has suggested both regulatory/anti-inflammatory properties and deleterious/pro-inflammatory effects of NO [79-81], *in vivo* evaluation of medical implants with physiologically-relevant NO fluxes have consistently found notably reduced tissue inflammation around the implant site [82-84]. Though the mechanisms are not completely understood, evidence suggests that NO influences FBR in various ways. Nitric oxide reduces inflammatory cell migration/recruitment to the device-tissue interface during the acute inflammatory response, subsequently reducing FBR. Localized NO is believed to inhibit cytokine and chemokine expression via nitrosation of relevant proteins. Further, NO is well-documented as an angiogenic agent during tissue reconstruction and is thus helpful for avoiding avascular encapsulation [85, 86]. Meanwhile, angiogenic factors, such as VEGF and transforming growth factor β, stimulate NO generation. Since NO also enhances VEGF synthesis, it may upregulate VEGF via a positive feedback loop [87]. The microbial infections associated with subcutaneous implantation can also be inhibited by NO owing to its potent antimicrobial activity [88, 89]. Therefore, a locally enhanced level of NO, given its multiple physiological functions, is expected to facilitate the exchange of glucose and other analytes into blood or subcutaneous fluid adjacent to the implanted sensor, thereby improving sensor performance.

This article is protected by copyright. All rights reserved

Author Manuscript

The nitric oxide release technology has been adopted for the development of many implantable devices, including both intravascular and subcutaneous electrochemical sensors, and has demonstrated favorable *in vivo* performance in preventing platelet activation/adhesion, thrombus formation, as well as providing anti-inflammatory effects and inhibiting bacterial cell proliferation and biofilm formation [72, 88, 90-92]. However, a major challenge limiting the application of NO release is the molecule's innate high reactivity with several *in vivo* species (e.g., oxyhemoglobin, thiols and oxygen), resulting in its very short life once in the bloodstream (< 1s) [93-94]. The reactivity and gaseous nature of NO makes it difficult to realize prolonged local delivery of NO at a high flux. This is especially true for miniaturized implantable sensors, as the effective loading of NO donors by entrapping or covalent attachment is inherently restricted since thicker coatings containing the NO donor will yield much slower sensor response times. According to previous studies, effective biocompatibility enhancement is only observed if NO release can be sustained for extended periods in or above the range of 0.5 to 4.0×10^{-10} mol cm^{-2} min^{-1}, a flux that mimics those produced by endothelial cells [13, 95].

2.2 Nitric oxide releasing/generation methods

The development of NO releasing methods that provide sufficient surface fluxes and duration (i.e., the amount of time when the NO flux is within or greater than the physiologically relevant range) is the key to fabricate more biocompatible *in vivo* sensors. Indeed, higher fluxes with longer duration of NO release generally correspond to improved *in vivo* device performance [13, 72, 88, 90-92]. This is especially true for intravascular sensors where oxy-Hb in blood will react rapidly with the NO released [96]. Furthermore, the NO releasing chemistry should not interfere with the sensing technology or chemistry used within the device. In particular, since NO is an electroactive species, it needs to be confirmed *in vitro* that the NO released is compatible with the working mechanism of the underlying electrochemical sensor so that the sensitivity and analytical signal are not significantly altered. To date, several different NO generating approaches have been reported for implantable sensors and illustrated in multiple review articles [16, 90]. These include coating/covalently attaching N-diazeniumdiolate or S-nitrosothiol (RSNO) species to sensors or sensing catheter surfaces, catalytically generating NO *in situ* from endogenous RSNOs using embedded metal ion-based catalysts, and electrochemically modulated NO generation from inorganic nitrite (Fig. 2). In addition to physically dispersed NO donors/vehicles within a polymer matrix, there has also been rapid development of NO releasing polymers (i.e., polymeric NO donors) with covalently bound NO donating groups. However, to date, few of these newer materials have been implemented in preparation of implantable sensors.

This article is protected by copyright. All rights reserved

Author Manuscript

N-diazeniumdiolates are NO adducts with secondary amines, and one of the most frequently investigated classes of NO donors. To form the corresponding diazeniumdiolate, one equivalent of secondary amine is reacted with two equivalents of gaseous NO under high pressure (e.g., 80 psi) [97]. Via a proton-driven reaction, each diazeniumdiolate molecule can degrade to release two equivalents of NO spontaneously along with the regenerated parent amine. The rates of NO production depend on pH, temperature, and the chemical structure of the precursor amine [98, 99]. N-diazeniumdiolates, either in molecular forms or as sol-gel particles, are commonly mixed into a polymer outer coating of implantable sensors to release NO. However, it remains a challenge to realize long-term (> 3 d) NO release at physiological levels using this approach. In addition, diazeniumdiolates are considered toxic via possible nitrosamine formation (via back-reaction of the NO with the amine), if the amine species can leach from the implanted device into blood or solution [100].

An attractive alternate class of NO donors are *S*-nitrosothiols (RSNO) [101-102]. Synthetic variants of RSNOs can be readily obtained by reaction of organic thiol species with nitrosating reagents. Indeed, one of the most popular RSNO species for use as an NO donor is *S*-nitrosoglutathione (GSNO), which is an endogenous transporter of NO in blood [103]. Another commonly used RSNO is *S*-nitroso-N-acetylpenicillamine (SNAP) whose precursor, N-acetylpenicillamine (NAP), has been approved by FDA as a drug to treat heavy metal poisoning [104]. RSNOs decompose readily via thermal and photolytic cleavage of the S-N bond to yield NO and a thiyl radical [105]. It was also found that several transition metal ions (most notably Cu^{+} species) can catalyze RSNO decomposition via irreversible catalytic redox reactions to accelerate the liberation of NO [106-107]. Furthermore, NO generation from RSNO can be mediated by ascorbate by way of two distinct pathways, depending on ascorbate concentrations [107]. RSNOs are also traditionally mixed in polymeric coatings of implantable devices in molecular forms, though they are increasingly being incorporated via sol-gel particles [108, 109], solvent impregnation [82, 110], and filling into cavities of devices in solid-state or solution [111, 112] to achieve extended NO release.

Another NO releasing method is the catalytic generation of NO at the surface of an implanted sensor from endogenous NO donors in blood such as *S*-nitrosated forms of serum albumin, *S*-nitrosocysteine, *S*-nitrosoglutathione, and nitrite. As such, this passive NO release would not depend on the amounts of donors entrapped in coatings on the sensing device and the biocompatibility benefit exists as long as there is adequate levels of these endogenous donors in its (the sensor's) microenvironment. Various groups of metal ion-based catalysts have been embedded within or covalently bonded to polymer coatings of medical implants for *in situ* catalytic generation of NO from endogenous RSNOs. These include copper(II) complexes [113, 114], organoselenium species [115], organoditelluride species [116], metal-organic frameworks (MOF) [117], and

Author Manuscript

This article is protected by copyright. All rights reserved

copper particles [118]. However, since this method depends on the level of endogenous NO donors in the blood or subcutaneous fluid, levels of NO generation/release can be inconsistent due to the variability in the levels of RSNOs present in blood and tissue.

Electrochemical generation of NO via electrocatalytic reduction of nitrite (NO_2^-), is another very promising method to produce highly controllable NO generation levels over a prolonged time period [119-121] while avoiding the leaching of NO donors and/or byproducts into the bloodstream. This "on-demand" NO generation approach allows easy control of the NO release level by adjusting the applied potential or current to a noble metal electrode (e.g., gold, platinum) and a Ag/AgCl reference electrode placed into the nitrite solution within one lumen of a multi-lumen catheter-type sensor. To effectively produce NO, water soluble copper(II)-ligand catalysts are continually being developed to electrochemically reduce nitrite in buffered aqueous solutions as the reaction medium [122, 123]. The longevity of NO release depends on the volume and concentration of nitrite within a catheter lumen reservoir attached to the sensor.

3. Current designs for NO releasing electrochemical sensors

3.1 NO releasing ion, oxygen and carbon dioxide sensors

The first NO releasing electrochemical sensors were reported by Espadas-Torre et al. [66]. In this early study, classic ionophore-based polymeric pH and K^+ sensing electrodes were prepared with N, N'-dimethylhexanediamine NO adduct (DMHD/N_2O_2) as an NO donor within a traditional ion-selective sensing membrane. This membrane also contains the ionophores (e.g., tridodecylamine for H^+, valinomycin for K^+), a polymer matrix (poly(vinyl chloride)), water-immiscible plasticizers and a suitable lipophilic ion-exchanger. The polymer film continuously releases low levels of NO from the DMHD/N_2O_2 species, while serving simultaneously as an analytical transducer for potentiometric selective ion sensing. NO release did not interfere with the ion-sensing chemistry, as evidenced by nearly identical Nernstian potentiometric responses/slopes and ion-selectivity over Na^+ from electrodes prepared with and without the incorporation of NO donors. After exposure to platelet-rich sheep plasma, thrombogenicity evaluation revealed significantly reduced platelet adherence and activation on NO releasing ion sensing films compared to the non-NO-releasing controls. The compatibility between NO release from the diazeniumdiolate species and potentiometric ion detection suggested potential benefits of NO release to a variety of biocompatible *in vivo* electrochemical sensors.

This article is protected by copyright. All rights reserved

Author Manuscript

Clark-type electrochemical (amperometric) O_2 sensors have previously been fabricated using an intravascular (IV) catheter (e.g., silicone rubber) configuration. In another early effort, Mowery et al. [124] reported the first NO releasing catheter-type amperometric oxygen sensors along with potentiometric pH and K^+ sensors with three distinctly different types of diazeniumdiolate NO donors, (Z)-1-{N-methyl-N-[6-(N-methylammoniohexyl)amino]}diazen-1-ium-1,2-diolate (MAHMA/N_2O_2) (note: MAHMA/N_2O_2 is the same molecule as DMHD/N_2O_2), linear polyethylenimine/N_2O_2 (LPEI/N_2O_2) and methoxymethyl piperazine polyvinyl chloride/N_2O_2 (mompipPVC/N_2O_2). These NO donors, after being mixed in PVC or PU polymer coatings on the sensing catheters, could release NO for extended periods of time (> 48 h), which led to a dramatic decrease in platelet adhesion and activation *in vitro*. The sensors with concomitant NO release exhibited device functionality analogous to blank control sensors. Moreover, the authors did not notice any increase in baseline current upon release of the physiological levels of NO. Such results confirmed that at the operating applied potential of the Clark-style oxygen sensors (–0.6 V vs. Ag/AgCl), the possible accumulation of NO and its oxidation product (e.g., nitrite) in the internal filling solution of such catheter-type PO_2 sensors at low levels of continuous NO release, has very limited effect on the accuracy of the oxygen measurement.

The first work to assess the *in vivo* analytical performance of NO-modified amperometric IV oxygen sensors was conducted by Schoenfisch et al. [125]. Gas permeable coatings formulated with cross-linked silicone rubber (SR) and NO-generating MAHMA/N_2O_2 species were dip-coated on a PO_2 sensing catheter prepared with silicone catheter tubing (with platinum and Ag/AgCl electrodes immersed in a 0.15 M KCl and 1.5% (wt) Methocel electrolyte solution inside the tubing). The sensors, modified by surface coating with MAHMA/N_2O_2-SR films, could emit NO at physiological levels for over 20 h. Neither sensitivity nor response time was affected by the addition of the NO donor. When tested in carotid and femoral arteries of mongrel dogs for 6–24 h in the absence of systemic anticoagulation, the IV NO-releasing PO_2 sensing catheters yielded output signals that closely followed the actual blood PO_2 values within 10% for the first 18 h. This superior overall sensor performance was in sharp contrast to the erratic readings of the control sensors (up to 50% deviation). The improvement in accuracy for the NO releasing sensors correlated with reduced *in vivo* platelet adhesion and thrombus formation. Despite the improved sensor accuracy and biocompatibility, one major concern was the leaching of NO donor and its decomposition products (DMHD and potentially its corresponding toxic nitrosamine) into blood. Therefore, new diazeniumdiolates of higher lipophilicity or covalently bound to the polymer membrane were proposed by the authors as potential solutions. Indeed, in a follow-up study, Frost et al. [126] developed a DACA-6/N_2O_2 diazeniumdiolate species covalently anchored to a silicone rubber polymer matrix to eliminate the problem of diamine and nitrosamine leaching. The Clark-

Author Manuscript

This article is protected by copyright. All rights reserved

type amperometric oxygen-sensing catheters coated with an outer layer of the DACA-6/N_2O_2 polymer could release endothelial levels of NO (> 1×10^{-10} mol min^{-1} cm^{-2}) for at least 20 h. Significantly improved analytical performances and effective inhibition of clot formation for the NO releasing sensors compared to control sensors, were also reported via IV tests within the carotid and femoral arteries of swine over a 16-h time period.

In addition to covalently tethering diazeniumdiolates to the polymer backbone, they can be directly generated on macromolecular scaffolds such as amine-based silica nanoparticles. Marxer et al. [127] designed a new amperometric sol–gel derived NO releasing oxygen sensor that offers prolonged NO release. To fabricate the sensor, a platinum (Pt) working electrode was first coated with aminosilane/ethyltrimethoxysilane hybrid xerogel film. The modified electrode was then doped with hydrophilic polyurethane (HPU) to reduce sensor hydration time and increase oxygen permeability, and subsequently exposed to 5 atm of high pressures NO gas for 3 d to form diazeniumdiolate groups. The sensors were then characterized and found to be highly sensitive to oxygen within a physiologically relevant range and exhibited rapid response times, and linear, repeatable amperometric signals. The NO flux was 4.3×10^{-10} mol min^{-1} cm^{-2} over the first 12 h and remained detectable through 48 h, effectively doubling the NO release time previously reported [125, 126]. Evaluated by a standard *in vitro* assay, the platelet adhesion was found to be minimal for at least 24 h on the NO releasing HPU-doped xerogel films, though the performance of such the PO_2 sensors still needs to be assessed *in vivo* given the presence of additional NO scavengers in the body (e.g., proteins, thiols, transition metals, etc.).

Due to the toxicity of diazeniumdiolate species via possible nitrosamine formation and leaching, various other NO generating strategies have been explored for preparation of intravascular PO_2 sensors. Wu et al. [128] adapted the concept of catalytic conversion of endogenous *S*-nitrosothiols (present in blood) to NO to prepare intravascular oxygen sensors. In this work, NO releasing catheter-type amperometric oxygen sensors were prepared by coating the catheter probes with polyurethane or polyurethane/silicone rubber layer doped with 3 nm or 80 nm Cu^0 particles. A slow corrosion of the copper particles in such polymer coatings produces Cu(II) ions that can catalyze the decomposition of GSNO (an endogenous RSNO in blood), so that physiological levels of NO can be generated *in situ* at the sensor/blood interface. The largely inhibited thrombus formation by NO, as found after 19–20 h of *in vivo* examination of the sensors in porcine arteries, significantly improved oxygen sensing accuracy compared to control sensors without the Cu^0 particles as catalysts. However, the authors also noticed that low RSNO levels in some animals could render the NO level insufficient to completely eliminate thrombus formation, which might negatively impact the practical use of this approach for enhancing the accuracy of *in vivo* sensors.

This article is protected by copyright. All rights reserved

Author Manuscript

In addition to utilizing endogenous RSNO species naturally present in blood, synthetic RSNOs been intensively investigated as NO donors to achieve extended release and lower donor leaching/toxicity for developing NO releasing intravascular chemical sensors. For example, in a recent work, McCabe et al. [129] prepared a simplified NO releasing IV amperometric oxygen sensor by solvent impregnating *S*-nitroso-N-acetylpenacillamine (SNAP) directly into the walls of a single-lumen silicone tube. The tubing was sealed at one end, filled with 0.15 M KCl in bicarbonate/carbonate buffer, and a Pt wire working electrode and Ag/AgCl reference electrode were placed into the inner solution to create an NO releasing catheter-type amperometric oxygen sensor. With the NO donor reservoir in the sensor wall, the SNAP-impregnated sensor is able to releases NO under physiological conditions ($> 0.5\times 10^{-10}$ mol min^{-1} cm^{-2}) for 18 d. By using rabbit and swine models over 7 and 20 h animal experiments (with sensors placed in both veins and arteries), the largely clot-free SNAP-impregnated PO_2 sensors exhibited deviations within ±15% of the true oxygen level for all time points (n=6, $p < 0.2$ at each time point), while control sensors showed > 20% deviation after only 5 h of *in vivo* testing (n=6, $p < 0.05$) due to much more severe thrombus formation.

Nitric oxide generation via electrochemical reduction of nitrite ions is an "on-demand" method to produce highly controllable levels of NO and to prevent leaching of NO donors and/or byproducts into the bloodstream. Ren and coworkers [130] were the first to combine this NO generating/releasing approach in an IV dual-lumen catheter-type amperometric oxygen sensor configuration and studied the *in vivo* performance of this sensor (Fig. 3(a)). To fabricate the sensor, one lumen of this dual-lumen PO_2 sensor was filled with a solution containing inorganic nitrite ions and a copper(II)-ligand complex (e.g., copper(II)-tri(2-pyridylmethyl)amine (Cu(II)TPMA)), as a catalyst for electrochemical reduction of nitrite at −0.4V. The second lumen was used as a conventional amperometric PO_2 sensor (using Pt wire and Ag/AgCl reference). The amperometric PO_2 sensing was found to be fully compatible with the NO released ($> 1.0 \times 10^{-10}$ mol cm^{-2} min^{-1} for more than 72 h), as no noticeable amperometric signal changes were observed with NO release at physiological flux levels. The IV sensors were then implanted in both veins and arteries of rabbits and pigs for up to 21 h for the evaluation of their *in vivo* analytical performance. The NO releasing sensors exhibited much less clot formation (~63% of reduction versus control catheters) (Fig. 3(b)) and more accurate analytical results (a relative average deviation of −2 ± 11% and 96% of the measurements within ±20% error) compared to the control sensors (a relative average deviation of −31 ± 28% and only 32% of the measurements within ±20% error), as shown in Fig. 3(c). The authors proved that the flux of the NO release from the device surface could be easily modulated or turned "on" and "off" by applying different voltages to the inner working wire electrode in the NO generating lumen, while the duration of NO generation/release can also be adjusted by changing

This article is protected by copyright. All rights reserved

Author Manuscript

the volume or concentration of nitrite within the reservoir. Overall, electrochemical NO generation has significant potential for improving the biocompatibility of implantable chemical sensors. Additional copper(II)-ligand complexes are being developed to realize improved efficiency when using lower nitrite concentrations and less sensitivity to oxygen levels [122, 123]. Meanwhile, the multi-lumen configuration requirement for the separate nitrite filling solution still needs to be proven feasible for other sensor types (e.g., ion, glucose, lactate). At the same time, this additional lumen to generate the NO electrochemically from nitrite increases the overall size of the implanted sensor. However, this may be acceptable since the electrochemical NO release approach would not have any risk of leaching of organic NO donors (or product species) into the blood/tissue.

Blood PCO_2 monitoring is of tremendous clinical value, as hypercapnia (elevated CO_2 levels) from respiratory failure is common in intensive care units (ICU) and is closely associated with severe conditions (e.g., chronic obstructive pulmonary disease, central nervous system depression, neuromuscular disorders, thoracic deformities, etc.). As a variant of the Stow-Severinghaus CO_2 sensor configuration, catheter-type potentiometric carbon dioxide sensors have demonstrated potential for intravascular applications when tested in heparinized animals [131, 132]. However, there has been a problem to endow the catheter-type CO_2 sensors with NO releasing ability, as the direct deposition of an NO releasing outer coating on the surface of such CO_2 sensors can disrupt the PCO_2 sensing chemistry due to the diffusion of NO donor and solvent into the pH-ionophore doped inner wall. Zhang et al., [133] recently addressed this issue by reporting the first intravascular NO releasing potentiometric carbon dioxide sensor (Fig. 4). Similar to previously reported dual lumen silicone catheter tubing configurations for PCO_2 sensing, the inner wall is doped with a proton ionophore tridodecylamine, a sodium tetrakis[3,5-bis(trifluoromethyl)phenyl]-borate (NaTFPB) cation-exchanger, and a nitrophenyloctylether (NPOE) plasticizer, as the H^+-sensitive membrane. When one lumen is filled with a bicarbonate/sodium chloride solution and the other with a strong 4-morpholinoethanesulfonic buffer (pH = 5.7), the voltage across the inner wall between the two lumens changes in proportion to the log PCO_2 in the surroundings, due to the equilibrium partitioning of CO_2 into the bicarbonate inner filling solution and subsequently increased proton activity in this solution (i.e., lowered pH) (note: for the mechanism of this novel dual lumen PCO_2 sensor, please see the Supporting Information in [133]). In addition, the dual lumen device is encapsulated within a thin SNAP-doped silicone tube that releases physiological levels of NO ($> 0.5 \times 10^{-10}$ mol cm^{-2} min^{-1}) for at least 7 d. Both the NO releasing sensors and controls exhibit good reversibility and near-Nernstian sensitivity to PCO_2 at 37°C, without any significant difference in the slopes (59.31 ± 0.78 mV/decade vs. 59.25 ± 0.71 mV/decade). *In vivo* studies were performed by testing sensors in both the arteries

This article is protected by copyright. All rights reserved

Author Manuscript

and veins of anesthetized pigs for 20 h. The data shows significant clot-reduction and enhanced accuracy for the NO releasing PCO_2 probes (vs. non-NO releasing controls) (Fig.5(a) and (b)). Continuously monitored PCO_2 values by NO releasing arterial and venous sensors correlated well with discrete *in vitro* blood gas analyzer values throughout the 20 h, with 93.3% and 89.4% of measurements falling within ±20% error, compared to 66.3% and 62% by control sensors, respectively (Fig. 5(c)). The PCO_2 catheter type probes also reported in this work represent the first potentiometric intravascular NO releasing sensors, as no *in vivo* data had been garnered with any of the prior efforts reporting on NO releasing potentiometric pH or ion-sensors.

3.2 NO releasing glucose and lactate sensors

Currently, most implantable continuous glucose monitoring (CGM) amperometric sensors measure glucose levels in interstitial fluid of subdermal tissues for tight glycemic control. NO release is a potential means to further mitigate foreign body response (FBR) and improve subcutaneous glucose sensor performance. The most common glucose sensors have been ones that rely on amperometric monitoring (at +0.6–0.7V) of hydrogen peroxide (H_2O_2), produced by the immobilized glucose oxidase (GOx) catalyzed reaction of glucose and natural oxygen substrate [134, 135]. This type of sensor is usually fabricated by coating a noble metal (e.g., Pt) working electrode with an interferent exclusion layer, an active catalytic GOx enzyme layer, followed by an outermost polymeric diffusion-limiting layer (to limit the diffusion of glucose relative to oxygen) [136]. Based on this design, Gifford et al. [137] developed the very first NO-releasing needle-type enzyme-based amperometric glucose sensors for subcutaneous glucose measurements. To realize NO release, the lipophilic diazeniumdiolate species, (Z)-1-[N-methyl-N-[6-(N-butylammoniohexyl)amino]]-diazen-1-ium-1,2-diolate (DBHD/N_2O_2), was further incorporated in the outer coating of polyurethane/polydimethylsiloxane (PU/PDMS). Despite the relatively short NO release time (16 h), the sensors exhibited excellent sensitivity, linear range and response time *in vitro*. The Clarke error grid correlation of sensor glycemia estimates versus blood glucose measured when the sensors were implanted subcutaneously in Sprague-Dawley rats was superior for the NO-releasing sensors when compared to controls on both days 1 and 3, with the NO releasing sensors also showing a reduced run-in time of minutes versus hours for control sensors. Histological examination of the implant site also suggested 100% of reduced inflammatory response for the NO releasing sensors within 24 h. However, the authors pointed out that a thicker PU outer-most layer with additional DBHD/N_2O_2 loading will likely change its permeability characteristics, and this would thus be detrimental to the sensitivity and response time of the glucose sensor.

This article is protected by copyright. All rights reserved

Author Manuscript

Therefore, the focus of subsequent studies in this area was to achieve an ideal balance between sustainable NO release, minimal leaching and good sensor performance.

Shin et al. [138] developed a hybrid NO donor modified sol-gel particle-doped polyurethane for electrochemical glucose sensor fabrication. This new NO releasing layer was sandwiched between two polyurethane layers on top of a GOx coated Pt working electrode. The synthesized aminosilane-based sol–gel particles were converted to diazeniumdiolates via exposure to high pressures of NO in an in-house NO reactor for 3 d before being mixed into a PU coating solution. The *in vitro* testing showed good sensitivity, reproducibility and fast response time to glucose (comparable to non-NO releasing control sensors). However, with this new sensor design, leaching of sol–gel particles and a reduction of sensitivity (due to enzyme inactivation) were still observed. Meanwhile, a longer-term NO release (> 1-2 days at or above physiological levels as reported in this study) is still desired for any miniaturized version of this sensor for evaluation of *in vivo* biocompatibility and analytical performance.

Oh et al. [139] reported an amperometric glucose micro-biosensor modified with diazeniumdiolate-modified NO-releasing xerogel micro-patterned array to avoid significantly limiting glucose diffusion and compromised glucose sensitivity. The GOx was first immobilized in a methyltrimethoxysilane (MTMOS) xerogel layer on a Pt electrode, followed by a polyurethane/hydrophilic polyurethane protective layer. Next, micropatterned xerogel lines (5 um wide) separated by distances of 5 or 20 um were formed on top to provide NO-release for 48 h (~ 0.9×10^{-10} mol cm^{-2} min^{-1} during initial hours). This microarray design enabled increased glucose sensitivity as only a small portion of the surface is modified by the NO release coating. The authors found that the levels of NO generated from such a design were still sufficient to reduce over 40% of platelet adhesion and 70–80% of *Pseudomonas aeruginosa* bacterial growth after 3 d, without compromising enzymatic activity of GOx. However, the NO release from the sensor needs to be extended beyond 48 h for longer-term *in vivo* testing of such miniaturized glucose sensors. In follow-up studies, Schoenfisch et al. [140] prepared NO-releasing xerogel membranes as coatings for an electrochemical glucose biosensor. Hydrophilic poly(vinylpyrrolidone) (PVP) was mixed into the GOx-containing xerogel membrane followed by the conversion of amine groups to diazeniumdiolate NO-donors (by exposure to 5 atm NO for 1–48 h). The sensor provided a way to improve permeability of both hydrogen peroxide and glucose, to ensure adequate response times and sensitivity. However, the NO release only lasted for about 12 h and in the absence of an additional top-coat, and concurrent leaching of the GOx sensing element led to a decrease in signal intensity and narrowing of the linear range. Koh et al. [141] further designed a polyurethane-based implantable glucose sensor modified by NO-releasing porous fiber mat (540 ± 139 nm fiber diameter, 94.1 ± 3.7% porosity). The

Author Manuscript

This article is protected by copyright. All rights reserved

fibers were spun from a solution of NO releasing 1,2-Epoxy-9-decene (ED)-functionalized fourth-generation poly(amidoamine) (PAMAM) dendrimers (PAMAM G4-ED/NO) and PU. The stable fiber structure was found to release ~100 nmol of NO per mg of polyurethane over 6 h without leaching of the NO donor, even in serum. Despite the interesting design, the *in vivo* analytical performance of this sensor has yet to be assessed.

In a different study, Koh et al. [142] reported how a series of different diazeniumdiolate and RSNO-based NO-releasing silica nanoparticles, when used to fabricate glucose sensors, could affect NO fluxes and delivery totals as well as sensor characteristics (e.g., response time, sensitivity and dynamic range). Using similar sensor designs, Soto and coworkers [143] in the same research group subsequently performed the first long-term (10 d) *in vivo* study on percutaneously implanted NO-releasing amperometric glucose sensors in swine. The effect of NO release duration on needle-type glucose sensor performance was studied using a PU outer coating doped with two different macromolecular NO release systems: N-diazeniumdiolate NO donors and S-nitrosothiol-modified silica nanoparticles of 3-methylaminopropyltrimethoxysilane (MAP) and 3-mercaptopropyltrimethoxysilane (MPTMS), MAP3/NO and MPTMS-RSNO, designed to release 99% of similar total NO payload (3.1 μmol cm^{-2}) for rapid (16.0 ± 4.4 h) or slower (>74.6 ± 16.6 h) durations, respectively. According to the data presented, the analytical performance of MAP3/NO-based sensors in terms of response time and both numerical and clinical accuracy was mostly superior to those of the MAP3 (control) and slower NO-releasing sensors, but this advantage decreased at implant periods beyond 3 days (i.e., days 7 and 10). In contrast, MPTMS-RSNO-based sensors with a slower and extended NO release profile, were characterized by better overall numerical glucose accuracy over the 10-d test period as well as shorter sensor lag times (<4.2 min) in response to intravenous glucose tolerance tests versus burst NO-releasing and control sensors (>5.8 min) at 3, 7, and 10 d. The fact that both rapid and slower NO-release sensors exhibited improved accuracy vs. controls, and such an improvement closely correlated with the periods of active NO release, suggests that the ultimate NO-release strategy could benefit from higher NO fluxes for even longer durations (i.e., several weeks).

Soto et al. [144] further designed an implantable glucose sensor with an HP-93A-100 PU membrane mixed with RSNO-modified silica nanoparticles as glucose diffusion-limiting outer layer. A linear glucose calibration between 1 and 21 mM was observed for over 2-weeks in PBS. Further, these extended NO-releasing sensors (> 0.48 $\times 10^{-10}$ mol min^{-1} cm^{-2} for up to 6 d) as well as low particle leaching (<0.6%) hold promise for mitigating the FBR and improving *in vivo* sensor functionality. Indeed, in a recent report, Malone-Povolny et al. [145] used a similar approach to fabricate an implanted needle-type amperometric glucose sensor to detect interstitial glucose. The surface modification layers included an electropolymerized selectivity

This article is protected by copyright. All rights reserved

Author Manuscript

layer, a sol−gel enzyme (GOx) layer, an NO releasing polyurethane layer doped with either nonporous (14 d release) or porous (30 d release) RNSO derivatized silica nanoparticles, and a polyurethane topcoat (Fig. 6(a)). Analytical performance and tissue interactions of the NO-releasing sensors were evaluated for as long as 28 d in a diabetic swine model. As expected, numerical and clinical accuracy of glucose detection and reduced FBR-associated inflammatory biomarkers over a time period were directly correlated with active NO release from the surface of subcutaneous glucose sensors. Notably, the porous silica particle-doped sensors that released NO for 30 d ($> 0.5 \times 10^{-10}$ mol cm^{-2} min^{-1} for at least 14 d and $> 0.18 \times 10^{-10}$ mol cm^{-2} min^{-1} on the 30th day) showed standard-compliant accuracy (i.e., MARD ≤ 15%) for >3 weeks post-implantation (Fig. 6(b)). The observed performance improvement was attributed to the NO providing a decrease of inflammatory cell count and a lower density collagen capsule. For subcutaneous NO releasing glucose sensors, extending the NO release beyond 30 d by new NO release strategies is a future goal to further mitigate the FBR and achieve adequate implantable sensor accuracy beyond 1 month.

Recently, intravascular glucose monitoring has been steadily gaining attention, as tight glycemic control has been shown to improve outcomes for ICU patients, with and without diabetes. Compared to subcutaneous glucose sensors, IV glucose sensors could circumvent the physiological delay between blood glucose and interstitial fluid glucose, though it has been proven challenging due to potential clot-formation at the blood/device interface. The anti-platelet properties of nitric oxide provide a new direction to address this issue. Early efforts in this direction were reported by the Meyerhoff research group. Yan et al. [146] developed a needle-type IV amperometric glucose sensors based on H_2O_2 detection and a layer of poly(lactide-co-glycolide) (PLGA) with NO releasing DBHD/N_2O_2 embedded within. The PLGA undergoes a slow hydrolysis process to produce lactic acid and glycolic acid, and thus provides an acidic local micro-environment for the proton-driven NO release from DBHD/N_2O_2 ($> 1 \times 10^{-10}$ mol cm^{-2} min^{-1} for at least 7 d). Clark error grid analysis shows that during *in vivo* experiments with sensors implanted in the veins of rabbits for 7 h, the NO releasing sensors had 97.5% of data points in Zone A (clinically accurate zone) and Zone B (benign error zone with no clinical consequences) while the value was 86.7% for the controls. Reduced thrombus formation was also evident for the NO releasing sensors. In a follow-up study by Wolf et al. [147], similar glucose sensors were fabricated except that DBHD/N_2O_2 was doped within the PLA coating instead of PLGA to activate the proton-driven NO release, which lasted for at least 7 d above 0.5×10^{-10} mol cm^{-2} min^{-1}. Further, E2As was selected as a replacement for the PurSil layer for potentially better biocompatibility and biostability (Fig. 7(a)). The accuracy and biocompatibility exhibited apparent improvement when such NO-releasing glucose sensors were assessed by implantation within rabbit veins for 7 h (Fig. 7(b) and (c)). However, these animal studies

Author Manuscript

This article is protected by copyright. All rights reserved

conducted to date are still preliminary. Longer experiment implant times with potentially better animal models are expected to confirm the true useful lifetime of such sensors in the bloodstream.

Cha et al. [148] were the first to demonstrate the compatibility of NO with implantable glucose dehydrogenase (GDH)-based amperometric glucose sensors using an osmium (III/II)-bipyridine-polyvinylimidazole complex to mediate electron transfer. A lower applied potential of +0.2 V required by this sensing chemistry to re-oxidize the mediator, compared to +0.6–0.7V required for the oxidation of H_2O_2 generated with GOx based sensors, minimizes the background current from oxidation of NO and oxidizable interferents at the underlying working electrode [149, 150]. Instead of coating an NO-releasing membrane on the enzymatic glucose sensing layer, the NO was released by surrounding SNAP-doped silicone tubing and subsequently diffused to the sensing surface, which circumvents additional blockage of glucose diffusion and simplified the sensor coating process. With a layer of Cu nanoparticles in the PU-based Carbosil polymer between the Teflon coating on the platinum–iridium working electrode and the SNAP-impregnated silicone tubing as catalysts, the NO release lasted for at least 3 d at physiological levels ($>1 \times 10^{-10}$ mol cm^{-2} min^{-1}). Though this design has not yet been evaluated *in vivo*, the excellent analytical results in PBS buffer and heparinized whole porcine blood at 37°C makes this new design promising for future IV studies.

The importance of detecting lactate concentrations in real-time is increasingly being recognized, as elevated lactate values are related to severe physiological conditions such as cardiogenic or endotoxic shock, respiratory failure, liver disease, and systemic disorders such as renal failure and tissue hypoxia [151-152]. Although glucose and lactate sensors share many commonalities in their designs, the inherent instability of enzymes used for lactate sensors, such as lactate oxidase (LOx) and lactate dehydrogenase (LDH), is a major problem for sensor construction. Yan et al., [146] proposed an IV lactate sensor design nearly identical to their glucose sensor counterpart. However, in spite of the addition of PEI to stabilize lactate oxidase, an apparent decrease of sensor response was observed for lactate sensors over a 7-d *in vitro* test period, likely due to LOx degradation. In a recent study, Wolf et al. [153] presented a wire-type LOx-based amperometric lactate sensor mounted within a dual-lumen catheter tethered to a wireless circuit module to monitor output data. SNAP, as an NO donor, was suspended within a silicone-based polymeric formulation and NO release through this catheter housing resulted in significant antimicrobial and anti-platelet/anti-thrombotic activity. Though the NO releasing sensor device was fully functional and *in vivo* continuous lactate measurements were performed intravascularly and subcutaneously for 10 h using a porcine model, the focus of this preliminary study was not on the benefit of *in vivo* NO release, as the animals were under systemic heparinization. Future animal

This article is protected by copyright. All rights reserved

Author Manuscript

studies are expected to employ non-heparinized animals to evaluate the combined analytical accuracy and anti-thrombotic properties of the NO-releasing sensor designs.

4. Conclusion and Perspectives

Nitric oxide releasing electrochemical sensors reported to date are summarized in Table 1. The research efforts toward optimizing NO release flux/longevity and electrochemical detection in these sensors have been extensive, especially when compared to the fairly limited reports on the corresponding fiber-optic based devices only for oxygen [154] and pH [155] detection. After nearly two decades of research on the implementation of NO releasing capability in such electrochemical devices, it can be concluded that NO is fully compatible with intravascularly and subcutaneously implanted electrochemical sensors, as its impact on sensor performance (sensitivity, selectivity, detection range, response time. etc.) is minimal with optimized sensor design considerations. Indeed, the active release of NO from the surface of sensors has been shown to directly correspond with improved numerical and clinical accuracy due to reduced adverse biological responses such as thrombus-formation/FBR-associated inflammatory responses in both *in vitro* and *in vivo* (animals) studies.

Therefore, NO release remains a promising strategy to potentially overcome the bottleneck for intra-arterial/intravenous measurements of blood gases and glucose, for which there has been very limited commercial success [15, 156]. However, almost all IV NO-releasing sensor studies reported to date have been restricted to < 24 h *in vivo* testing durations due to the concern of aggravated thrombosis and ensuing poorer performance over time. It thus remains unclear if NO-releasing sensors can remain essentially thrombus-free in the blood stream for extended implant times (>3 d for practical use), which could be the essential next step for research in this direction. Similarly, despite the immense success in commercial subcutaneous glucose monitoring systems in recent years, further NO release studies for longer periods of subcutaneous implantation (> 30 d) to prevent FBR-induced issues will be valuable toward the realization of the next generation CGM systems that could exhibit longer use-life and limited calibration requirements [19-21, 32, 36, 157, 158].

In recent years, much progress has been made to improve the NO payload and stability toward elongated NO releasing lifetime, owing to the new development and understanding of NO generating materials and methods. For instance, various NO releasing polymer substrates/implants could already deliver physiological levels of NO for weeks and even months [82, 109, 159-160]. Meanwhile, novel NO donors and macromolecular scaffolds are continuously being synthesized for even more prolonged and controlled NO delivery [90, 161-165]. Some of them have shown promises for fabricating the next generation NO-releasing

This article is protected by copyright. All rights reserved

Author Manuscript

electrochemical sensors. However, limited by the possible overall loading of NO, particularly in the membranes of miniaturized *in vivo* sensor devices, NO alone is unlikely to provide the ultimate solution for the entire biocompatibility problem. Given the inevitable decrease of NO fluxes over time, it will be appealing to explore a dynamic, multifaceted strategy that combines a number of agents/materials, to possibly mimic the non-thrombogenic surface of vascular endothelium and complement NO eluting sensor devices. In fact, considerable research efforts have been devoted to dual-/multi-functional polymeric coatings that combine NO release functionality with other active agents for increased efficacies, including anticoagulants (e.g., heparin) [166-168], direct thrombin inhibitors [169], antimicrobial metal ions [170], quaternary ammonium compounds [171], PEG [172], zwitterionic polymers [173], antibiotics [174], CD47 peptide [112], and nonsteroidal anti-inflammatory drugs (NSAIDs) [175]. However, in spite of the preliminary evidence that supports simultaneous use of complementary antithrombotic/anti-inflammatory methods, the development of such multi-functional approaches still has to be studied to ensure that there are no negative effects on detection mechanism for implantable NO releasing sensors, and that reliable long-term output signals can be truly realized *in vivo*.

Author Manuscript

Note

The authors declare no competing financial interest.

Acknowledgement

This work was supported by National Institutes of Health (Grant NIH-EB-023294).

Data Availability Statement

Data sharing not applicable- no new data generated

References

[1] G. S. Wilson, Y. Hu, *Chem. Rev.* **2000**, *100*, 2693– 2704.
[2] G. S. Wilson, R. Gifford, *Biosens. Bioelectron.* **2005**, *20*, 2399–2403.
[3] M. Frost M, M. E. Meyerhoff, *Curr Opin Chem Biol.* **2002**, *6*, 633–641.
[4] E. Fogt, *Clin. Chem.* **1990**, *36*, 1573-1580.
[5] M. E. Meyerhoff, *TrAC, Trends Anal. Chem*. **1993**, *12(6)*, 257− 266.
[6] J. W. Severinghaus, P. Astrup, J. F. Murray, *Am. J. Respir. Crit. Care Med.* **1998**, *157*, S114−S122.
[7] W. V. Tamborlane et al., *N. Engl J Med.* **2008**. *359(14)*, 1464-76.
[8] D. Rodbard, *Diabetes Technol Ther* **2016**, *18(Suppl. 2)*, S2–S13.

This article is protected by copyright. All rights reserved

[9] B. D. Ratner, *Biomaterials*, **2007**, *28(34)*, 5144-5147
[10] J. M. Anderson, A. Rodriguez, D. T. Chang, *Semin. Immunol*., **2008**, *20(2)*, 86-100.
[11] N. Wisniewski, F. Moussy, W.M. Reichert, *Fresenius J. Anal. Chem*. **2000**, *366*, 611–621.
[12] M. Frost, M. E. Meyerhoff, *Anal. Chem.* **2006**, *78*, 7370–7377.
[13] Y. Wu, M. E. Meyerhoff, *Talanta* **2008**, *75*, 642–650.
[14] B. D. Ratner, *J. Biomed. Mater. Res*. **1993**, *27(3)*, 283-287.
[15] M. C. Frost, M. E. Meyerhoff, *Annu. Rev. Anal. Chem*. **2015**, *8*, 171-192.
[16] R. J. Soto, J. R. Hall, M. D. Brown, J. B. Taylor, M. H. Schoenfisch, *Anal. Chem*. **2017**, *89*, 276−299.
[17] M. Ganter, A. Zollinger, *Br. J. Anaesth.* **2003**, *91(3)*, 397−407.
[18] C. K. Mahute, *Clin. Biochem.* **1998**, *31*, 119-130.
[19] J. M. Anderson, R. E. Marchant, in *Infections Associated with Indwelling Medical Devices* (Ed: F. A. Waldvogel, A. L. Bisno), ASM Press, Washington, DC, **2000**, 89–109.
[20] H. Teymourian, A. Barfidokht, J. Wang, *Chem. Soc. Rev*., **2020**, *49*, 7671-7709.
[21] R. J. Galindo, G. Aleppo, *Diabetes Res. Clin. Pract.*, **2020**, *170*, 108502.
[22] D. DeSalvo, B. Buckingham, *Curr Diab Rep.* **2013**, *13(5)*, 657–662.
[23] E. Cengiz, W. V. Tamborlane, *Diabetes Technol Ther.* **2009**, *11(Suppl 1)*, S11–S16.
[24] E. Kulcu, J. A. Tamada, G. Reach, R. O. Potts, M. J. Lesho, *Diabetes Care*, **2003**, *26(8)*, 2405-2409.
[25] E. M. Hetrick, H. L. Prichard, B. Klitzman, M. H. Schoenfisch, *Biomaterials* **2007**, *28*, 4571–4580.
[26] H. Lee, Y. J. Hong, S. Baik, T. Hyeon, D.-H. Kim, *Adv. Healthc. Mater*., **2018**, *7(8)*, 1701150.
[27] Y. Wang, S. Vaddiraju, B. Gu, F. Papadimitrakopoulos, D. J. Burgess, *J Diabetes Sci Technol.* **2015**, *9(5)*, 966–977.
[28] J. M. Anderson, *Cardiovasc Pathol*. **1993**, *2*, 33-41.
[29] M. Gerritsen, J. A. Jansen, J. A. Lutterman, *Neth. J. Med.* **1999**, *54*, 167–179.
[30] W. K. Ward, *J Diabetes Sci Technol* **2008**, *2*, 768-777.
[31] U. Klueh, D. I. Dorsky, D. L. Kreautzer, *Biomaterials* **2005**, *26*, 1155-1163.
[32] J. I. Joseph, G. Eisler, D. Diaz, A. Khalf, C. Loeum, M. C. Torjman, *Diabetes Technol Ther.* **2018**, *20(5)*, 321–324.
[33] G. Acciaroli, M. Vettoretti, A. Facchinetti, G. Sparacino, *Biosensors* **2018**, *8(1)*, 24.
[34] N. Wisniewski, M. Reichert, *Colloids Surf. B Biointerf.* **2000**, *18*, 197.
[35] Y. Onuki, U. Bhardwaj, F. Papadimitrakopoulos, D. J. Burgess, *J Diabetes Sci Technol* 2008, 2(6), 1003-1015.
[36] S. P. Nichols, A. Koh, W. L. Storm, J. H. Shin, M. H. Schoenfisch, *Chem. Rev.* **2013**, *113*(4,) 2528–2549.
[37] P.H. Kvist, H.E. Jensen, *J. Diabetes Sci. Technol.* **2007**, *1(5)*, 746–752.
[38] P. Lin, C. Lin, R. Mansour, F. Gu, *Biosens. Bioelectron*. **2013**, *47*, 451–460.
[39] A. J. T. Teo, A. Mishra, I. Park, Y. Kim, W. Park, Y. Yoon, *ACS Biomater. Sci. Eng.* **2016**, *2(4)*, 454–472.
[40] X. H. Wang, in *Advances in Biomaterials Science and Applications in Biomedicine* (Ed: R.Lazinica), InTech, Rijeka, Croatia, **2013**, 111–155.
[41] C. Espadas-Torre, M. Meyerhoff, *Anal. Chem.* **1995**, *67*, 3108–3114.
[42] C. Quinn, R. Connor, A. Heller, *Biomaterials* **1997**, *18*, 1665–1670.
[43] D. Grainger, *Nat Biotechnol* **2013**, *31*, 507–509.
[44] S. Abraham, S. Brahim, K. Ishihara, A. Guiseppi-Elie, *Biomaterials* **2005**, *26(23)*, 4767-4778.
[45] S. Zhang, Y. Benmakroha, P. Rolfe, S. Tanaka, K. Ishihara, *Biosens. Bioelectron.* **1996**, *11*, 1019–1029.
[46] B. Towe, V. Pizziconi, *Biosens. Bioelectron.* **1997**, *12*, 893–899.
[47] G. P. Rigby, P. W. Crump, P. Vadgama, *Analyst*, **1996**, *121*, 871-875
[48] G. P. Rigby, S. Ahmed, G. Horseman, P. Vadgama, *Anal. Chim. Acta* **1999**, *385*, 23–32.
[49] D.J. Harrison, R.F. Turner, H. P. Baltes, *Anal. Chem*. **1988**, *60*, 2002–2007.

Author Manuscript

This article is protected by copyright. All rights reserved

[50] F Moussy, D. J Harrison, R. V. Rajotte, *Int. J. Artif. Organs.* **1994**, *17(2)*, 88-94.

[51] M. Kyrolainen, H. Hakanson, B. Mattiasson, P.Vadgama, *Biosens. Bioelectron*. **1997**, *12*, 1073–1081.

[52] S. M. Reddy, P. M. Vadgama, *Anal. Chim. Acta* **1997**, *350*, 77–89.

[53] S. P. J. Higson, P. M. Vadgama, *Anal. Chim. Acta* **1993**, *271*, 125–133.

[54] S. P. J. Higson, P. M. Vadgama, *Anal. Chim. Acta* **1995**, *300*, 77–83.

[55] B. Yu, N. Long, Y. Moussy, F. Moussy, *Biosens. Bioelectron*. **2006**, *21(12)*, 2275-2282

[56] D. J. Martin, L. A. P. Warren, P. A. Gunatillake, S. J. McCarthy, G. F. Meijs, K. Schindhelm, *Biomaterials* **2000**, *21*, 1021-1029.

[57] H.P. Ammon, W. Ege, M. Oppermann, W. Gopel, S. Eisele, *Anal. Chem*. **1995**, *67*, 466–471.

[58] S. Pradhan, A. K. Brooks, V. K. Yadavalli, *Materials Today Bio*, **2020**, *7*, 100065.

[59] M. Aramesh, O. Shimoni, K. Fox, T. J. Karle, A. Lohrmann, K. Ostrikov, S. Prawer, J. Cervenkaaf, *Nanoscale*, **2015**, *7*, 5998-6006.

[60] Y. M. Ju, B. Yu, T. J Koob, Y. Moussy, F. Moussy, *J. Biomed. Mater. Res. A.* **2008**, *87(1)*, 136-146.

[61] J. Wang, L. Chen, S. B. Hocevar, B. Ogorev, *Analyst* **2000**,*125*, 1431-1434

[62] S. S. Praveen, R. Hanumantha, J. M. Belovich, B. L. Davis, *Diabetes Technol. Ther.* **2003**, *5(3),393-399.*

[63] S. G. Vallejo-Heligon, B. Klitzman, W. M. Reichert, *Acta Biomaterialia*, **2014**, *10(11)*, 4629-4638.

[64] U. Klueh, D. I. Dorsky, D. L. Kreutzer. *J Biomed Mater Res* **2003**, *67A(3)*, 1072–86.

[65] L. W. Norton, H. E. Koschwanez, N. A. Wisniewski, B. Klitzman, W. M. Reichert, *J. Biomed Mater Res A.* **2007** *81(4)*, 858-69.

[66] C. Espadas-Torre, V. Oklejas, K. Mowery, M. E. Meyerhoff, *J. Am. Chem. Soc.* **1997**, *119*, 2321–2322.

[67] G.-R. Wang, Y. Zhu, P. V. Halushka, T. M. Lincoln, M. E. Mendelsohn, *Proc. Natl. Acad. Sci. U.S.A.* **1998**, *95*, 4888−4893.

[68] J. W. Coleman, *Int. Immunopharmacol.* **2001**, *1*, 1397−1406.

[69] R. Korhonen, A. Lahti, H. Kankaanranta, E. Moilanen, *Curr. Drug Targets: Inflammation Allergy* **2005**, *4*, 471−479.

[70] J. MacMicking, Q. W. Xie, C. Nathan, *Annu. Rev. Immunol.* **1997**, *15*, 323−50.

[71] E. Änggård, *Lancet*, **1994**, *343 (8907)*, 1199-1206.

[72] K. H. Cha, X. Wang, M. E. Meyerhoff, *Appl. Mater. Today* **2017**, *9*, 589–597.

[73] C. Nathan, Q. W. Xie, *Cell*, **1994**, *78*, 915-918.

[74] A. R. Butler, D. L. H. Williams, *Chem. Soc. Rev*., **1993**, *22*, 233-241.

[75] R. Bruckdorfer, *Mol. Aspects Med*. **2005**, *26*, 3–31.

[76] A. Gries, C. Bode, K. Peter, A. Herr, H. Bohrer, J. Motsch, E. Martin, *Circulation* **1998**, *97*, 1481−1487.

[77] J. E. Freedman, J. Loscalzo, M. R. Barnard, C. Alpert, J. F. Keaney, A. D. Michelson, *J Clin Invest.* **1997**, *100(2)*, 350-356.

[78] G. Walford, J. Loscalzo, *J. Thromb. Haemostasis* **2003**, *1*, 2112−2118.

[79] T. J. Guzik, R. Korbut, T. Adamek-Guzik, *J. Physiol. Pharmacol*. **2003**, *54*, 469.

[80] E. M. Hetrick, M. H. Schoenfisch, *Annu. Rev. Anal. Chem.* **2009**, *2*, 409–433.

[81] M. B. Grisham, D. Jourd'Heuil, D. A. Wink, *Am J Physiol.* 1999, *276 (2)*, G315-321.

[82] X. Wang, A. Jolliffe, B. Carr, Q. Zhang, M. Bilger, Y. Cui, J. Wu, X. Wang, M. Mahoney, A. Rojas-Pena, M. J. Hoenerhoff, J. Douglas, R. H. Bartlett, C. Xi, J. L. Bull, M. E. Meyerhoff, *Biomater. Sci*. **2018**, *6*, 3189−3201.

[83] E. M. Hetrick, H. L. Prichard, B. Klitzman, M. H. Schoenfisch, *Biomaterials* **2007**, *28(31)*, 4571–4580.

[84] S. P. Nichols, A. Koh, N. L. Brown, M. B. Rose, B. Sun, D. L. Slomberg, D. A.Riccio, B. Klitzman, M. H.Schoenfisch, Biomaterials, **2012**, *33 (27)*, 6305-6312.

[85] Y. Wang, S. Chen, Y. Pan, J. Gao, D. Tang, D. Kong, S. Wang, *J. Mater. Chem. B* **2015**, *3*, 9212–9222.

[86] L. J. Taite, P. Yang, H. W. Jun, J. L. West, *J. Biomed. Mater. Res. B: Appl. Biomater.* **2008**, *84*, 108–116.

This article is protected by copyright. All rights reserved

Author Manuscript

[87] J. Dulak, A. Jozkowicz, A. Dembinska-Kiec, I. Guevara, A. Zdzienicka, D. Zmudzinska-Grochot, I. Florek, A. Wojtowicz, A. Szuba, J. P. Cooke, *Arterioscler., Thromb., Vasc. Biol.* **2000**, *20*, 659− 666.

[88] A. W. Carpenter, M. H. Schoenfisch, *Chem. Soc. Rev.* **2012**, *41*, 3742–3752.

[89] M. A. De Groote, F. C. Fang, *Clin. Infect. Dis.* **1995**, *2(Suppl 2)*, S162-165.

[90] Y. Wo, E. J. Brisbois, R. H. Bartlett, M. E. Meyerhoff, *Biomater. Sci*., **2016**, *4*, 1161-1183.

[91] S. P. Nichols, A. Koh, N. L. Brown, M. B. Rose, B. Sun, D. L. Slomberg, D. A. Riccio, B. Klitzman, M. H. Schoenfisch, *Biomaterials* **2012**, *33*, 6305–6312.

[92] M. C. Frost, M. M. Batchelor, Y. M. Lee, H. P. Zhang, Y. J. Kang, B. K. Oh, G. S. Wilson, R. Gifford, S. M. Rudich, M. E. Meyerhoff, *Microchem. J.* **2003**, *74*, 277–288.

[93] D, D. Thomas, X. Liu, S. P. Kantrow, J. R. Lancaster, *Proc. Natl. Acad. Sci. U.S.A.*, **2001**. *98(1)*. 355–360.

[94] M. Vaughn, L. Kuo, J. Liao, *J. Cell. Physiol.* **1998**, *274*, H2163–H2176.

[95] M. W. Vaughn, L. Kuo, J. C. Liao, *Am. J. Physiol. Heart Circ. Physiol.* **1998**, *274*, H1705–H1714.

[96] A. J. Gow, B. P. Luchsinger, J. R. Pawloski, D. J. Singel, J. S. Stamler, *Proc. Natl. Acad. Sci. U.S.A.*, **1999**, *96(16)*, 9027-9032.

[97] R.S. Drago, B. R. Karstetter, *J. Am. Chem. Soc.* **1961**, *83*, 1819–1822.

[98] L. K. Keefer, *ACS Chem. Biol.* **2011**, *6*, 1147−1155.

[99] K. M. Davies, D. A. Wink, J. E. Saavedra, L. K. Keefer, *J. Am. Chem. Soc.* **2001**, *123(23)*, 5473–5481.

[100] K. A. Mowery, M. H. Schoenfisch, J. E. Saavedra, L. K. Keefer, M. E. Meyerhoff, *Biomaterials* **2000**, *21*, 9–21.

[101] D. L. H. Williams, *Acc. Chem. Res.* **1999**, *32(10)*, 869–876.

[102] K. Szacilowski, Z. Stasicka, *Prog. React. Kinet. Mech*. **2001**, *26*, 1–58.

[103] S. P. Singh, J. S. Wishnok, M. Keshive, W. M. Deen, and S. R. Tannenbaum, *Proc. Natl. Acad. Sci. U.S.A.* **1996,** *93(25)*, 14428-14433.

[104] R. A. P. Kark, D. C. Poskanzer, J. D. Bullock, G. Boylen, *N. Engl. J. Med.* **1971**, *285 (1)*, 10−16.

[105] R. J. Singh, N. Hogg, J. Joseph, B. Kalyanaraman, *J. Biol. Chem.* **1996**, *271*, 18596–18603.

[106] C.W. McCarthy, R. J. Guillory, II, J. Goldman, M. C. Frost, *ACS Appl. Mater. Interfaces* **2016**, *8(16)*, 10128–10135.

[107] A. J. Holmes, D. L. H. Williams, *J. Chem. Soc., Perkin Trans. 2*, **2000**, 1639-1644.

[108] D. A. Riccio, K. P. Dobmeier, E. M. Hetrick, B. J. Privett, H. S. Paul, M. H. Schoenfisch, *Biomaterials* **2009**, *30(25)*, 4494–4502.

[109] M. J. Malone-Povolny, M. H. Schoenfisch, *ACS Appl. Mater. Interfaces* **2019**, *11(13)*, 12216–12223.

[110] Y. Wo, Z. Li, E. J. Brisbois, A. Colletta, J. Wu, T. C. Major, C. Xi, R. H. Bartlett, A. J. Matzger, M. E. Meyerhoff, *ACS Appl. Mater. Interfaces* **2015**, *7*, 22218−22227.

[111] J. C. Doverspike, S. J. Mack, A. Luo, B. Stringer, S. Reno, M. S. Cornell, A. Rojas-Pena, J. Wu, C. Xi, A. Yevzlin, M. E. Meyerhoff, *ACS Appl. Mater. Interfaces* **2020**, *12(40)*, 44475-44484.

[112] Q. Zhang, S. J. Stachelek, V. V. Inamdar, I. Alferiev, C. Nagaswami, J. W. Weisel, J. H. Hwang, M. E. Meyerhoff, *Colloids Surf., B* **2020**, *192*, 111060.

[113] B. K. Oh, M. E. Meyerhoff, *J. Am. Chem. Soc.* **2003**, *125*, 9552–9553.

[114] S. Hwang, W. Cha, M. E. Meyerhoff, *Angew. Chem. Int.* **2006**, *45*, 2745–2748.

[115] W. Cha, M. E. Meyerhoff, *Biomaterials* **2007**, *28*, 19–27.

[116] S. Hwang, M. E. Meyerhoff, *J. Mater. Chem.* **2007**, *17*, 1462–1465.

[117] M. J. Neufeld, A. Lutzke, W. M. Jones, M. M. Reynolds, *ACS Appl. Mater. Interfaces* **2017**, *9(41)*, 35628–35641.

[118] J. Pant, M.J. Goudie, S. P. Hopkins, E. J. Brisbois, H. Handa, *ACS Appl. Mater. Interfaces* **2017**, *9(18)*, 15254–15264

[119] H. Ren, J. Wu, C. Xi, N. Lehnert, T. C. Major, R. H. Bartlett, M. E. Meyerhoff, *ACS Appl. Mater. Interfaces* **2014**, *6*, 3779–3793.

[120] L. Höfler, D. Koley, J. Wu, C. Xi, M. E. Meyerhoff, *RSC Adv*., **2012**, *2*, 6765-6767.

Author Manuscript

This article is protected by copyright. All rights reserved

[121] V. Wonoputri, C. Gunawan, S. Liu, N. Barraud, L. H. Yee, M. Lim, R. Amal, *ACS Appl. Mater. Interfaces* **2015**, *7(40)*, 22148–22156

[122] A. P. Hunt, A. E. Batka, M. Hosseinzadeh, J. D. Gregory, H. K. Haque, H. Ren, M. E. Meyerhoff, N. Lehnert, *ACS Catal.* **2019**, *9(9)*, 7746–7758.

[123] K. K. Konopińska, N. J Schmidt, A. P Hunt, N. Lehnert, J. Wu, C. Xi, M. E Meyerhoff, *ACS Appl. Mater. Interfaces* **2018**, 10(30), 25047–25055.

[124] K.A. Mowery, M. H. Schoenfisch, N. Baliga, J. A. Wahr, M. E. Meyerhoff, *Electroanalysis* **1999**, *11*, 681–686.

[125] M. H. Schoenfisch, K. A. Mowery, M. V. Rader, N. Baliga, J. A. Wahr, M. E. Meyerhoff, *Anal. Chem.* **2000**, *72*, 1119–1126.

[126] M. C. Frost, S. M. Rudich, H. P. Zhang, M. A. Maraschio, M. E. Meyerhoff, *Anal. Chem.* **2002**, *74*, 5942–5947.

[127] S. M. Marxer, M. E. Robbins, M. H. Schoenfisch, *Analyst*, **2004**, *130*, 206–212.

[128] Y. Wu, A. P. Rojas, G. W. Griffith, A. M. Skrzypchak, N. Lafayette, R. H. Bartlett, M. E. Meyerhoff, *Sens. Actuators B* **2007**, *121*, 36.

[129] M. M. McCabe, P. Hala, A. Rojas-Pena, O. Lautner-Csorba, T. C. Major, H. Ren, R. H. Bartlett, E.J. Brisbois, M. E. Meyerhoff, *Talanta.* **2019**, *205*, 120077.

[130] H. Ren, M. A. Coughlin, T. C. Major, S. Aiello, A. R. Pena, R. H. Bartlett, M. E. Meyerhoff, *Anal. Chem.* **2015**, *87(16)*, 8067–8072.

[131] M. Telting-Diaz, M. E. Collison, M. E. Meyerhoff, *Anal. Chem.* **1994**, *66*, 576– 583.

[132] R. K. Meruva, M. E. Meyerhoff, *Biosens. Bioelectron.* **1998**, *13*, 201–212.

[133] Q. Zhang, G. P. Murray, J. E. Hill, S. L. Harvey, A. Rojas-Pena, J. Choi, Y. Zhou, R. H. Bartlett, M. E. Meyerhoff, *Anal. Chem.* **2020**, *92(20)*, 13641–13646.

[134] G. Guilbault, G. Lubrano, *Anal. Chim. Acta* **1973**, *64*, 439.

[135] J. Wang, *Electroanalysis*, **2001**, *13(12)*, 983-988.

[136] Y. Zhang, Y. Hu, G. S. Wilson, D. Moatti-Sirat, V. Poitout, G. Reach, *Anal. Chem.* **1994**, *66(7)*, 1183–1188.

[137] R. Gifford, M.M. Batchelor, Y. Lee, G. Gokulrangan, M.E. Meyerhoff, G. S. Wilson, *J. Biomed. Mater. Res. A* **2005**, *75*, 755–766.

[138] J. H. Shin, S.M. Marxer, M.H. Schoenfisch, *Anal. Chem*. **2004**, *76*, 4543–4549.

[139] B. K. Oh, M. E. Robbins, B. J. Nablo, M. H. Schoenfisch, *Biosens. Bioelectron*. **2005**, *21*, 749–757.

[140] M. H. Schoenfisch, A. R. Rothrock, J. H. Shin, M. A. Polizzi, M. F. Brinkley, K. P. Dobmeier, *Biosens. Bioelectron*. **2006**, *22*, 306–312

[141] A. Koh, Y. Lu, M. H. Schoenfisch, *Anal. Chem.* **2013**, *85*, 10488–10494.

[142] A. Koh, D. A. Riccio, B. Sun, A. W. Carpenter, S. P. Nichols, M. H. Schoenfisch, *Biosens. Bioelectron.* **2011**, *28*, 17–24.

[143] R. J. Soto, B. J. Privett, M. H. Schoenfisch, *Anal. Chem.* **2014**, *86*, 7141−7149.

[144] R. J. Soto, J. B. Schofield, S. E. Walter, M. J. Malone-Povolny, M. H. Schoenfisch, *ACS Sens.* **2017**, *2*, 140–150.

[145] M. J. Malone-Povolny, E. P. Merricks, L. E. Wimsey, T. C. Nichols, M. H. Schoenfisch, *ACS Sens.* **2019**, *4*, 3257–3264.

[146] Q. Yan, T. C. Major, R. H. Bartlett, M. E. Meyerhoff, *Biosens. Bioelectron*. **2011**, *26*, 4276–4282.

[147] A. K. Wolf, Y. Qin, T. C. Major, M. E. Meyerhoff, *Chin. Chem. Lett.* **2015**, *26*, 464–468.

[148] K. H. Cha, M. E. Meyerhoff, *ACS Sens.* **2017**, *2*, 1262–1266.

[149] T. J. Ohara, R. Rajagopalan, A. Heller, *Anal. Chem.* **1993**, *65*, 3512-3517.

[150] A. Heller, B. Feldman, *Chem. Rev.* **2008**, *108(7)*, 2482–2505.

[151] J. Bakker, M. W. N Nijsten, T. C Jansen, *Ann Intensive Care.* **2013**, *3*, 12.

[152] K. Rathee, V. Dhull, R. Dhull, S. Singh, *Biochem. Biophys. Rep*. **2016**, *5*, 35-54.

This article is protected by copyright. All rights reserved

Author Manuscript

[153] A. Wolf, K. Renehan, K. K. Y. Ho, B. D. Carr, C. V. Chen, M. S. Cornell, M. Ye, A. Rojas-Peña, H. Chen, *Biosensors*, **2018**, *8(4)*, 122.

[154] M. H. Schoenfisch, H. Zhang, M. C. Frost, M. E. Meyerhoff, *Anal. Chem.* **2002**, *74(23)*, 5937-5941.

[155] K. P. Dobmeier, G. W. Charville, M. H. Schoenfisch, *Anal. Chem.* **2006**, *78(21)*, 7461-7466.

[156] J. L. Smith, M. J. Rice, *J Diabetes Sci Technol.* **2015**, *9(4)*, 782–791.

[157] B. J. van Enter, E. von Hauff, *Chem. Commun*., **2018**, *54*, 5032-5045.

[158] S. G. Vallejo-Heligon, N. L. Brown, W. M. Reichert, B. Klitzman, Porous, *Acta Biomater.* **2016**, *30*. 106–115.

[159] E. J. Brisbois, H. Handa, T. C.Major, R. H. Bartlett, M. E. Meyerhoff, *Biomaterials* **2013**, *34(28)*, 6957-6966.

[160] S. P. Hopkins, J. Pant, M. J. Goudie, C. Schmiedt, H. Handa, *ACS Appl. Mater. Interfaces* **2018**, *10(32)*, 27316–27325.

[161] D. A. Riccio, M. H. Schoenfisch, *Chem Soc Rev.* **2012** *41(10)*, 3731–3741.

[162] T. Yang, A. N. Zelikin, R. Chandrawati, *Adv. Sci*. **2018**, *5*, 1701043.

[163] H. Liang, P.Nacharaju, A. Friedman, J. M Friedman, *Future Sci. OA* **2015** *1(1)*, FSO54.

[164] Y. Zhou, Q. Zhang, J. Wu, C. Xi, M. E Meyerhoff, *J. Mater. Chem. B,* **2018**, *6*, 6142-6152

[165] Y. Zhou, J. Tan, Y. Dai, Y. Yu, Q. Zhang, M. E Meyerhoff, *Chem. Commun*., **2019**, *55*, 401-404.

[166] R. Devine, M. J. Goudie, P. Singha, C. Schmiedt, M. Douglass, E. J. Brisbois, H. Handa, *ACS Appl. Mater. Interfaces*, **2020**, *12(18)*, 20158–20171.

[167] Z. R. Zhou, M. E. Meyerhoff, *Biomaterials*, **2005**, *26*, 6506-6517.

[168] B. Wu, B. Gerlitz, B.W. Grinnell, M. E. Meyerhoff, *Biomaterials* **2007**, *28*, 4047-4055.

[169] T. C. Major, E. J. Brisbois, A.M. Jones, M. E. Zanetti, G. M. Annich, R. H. Bartlett, H. Handa, *Biomaterials* **2014**, *35(26)*, 7271–7285.

[170] W. L. Storm, J. A. Johnson, B. V. Worley, D. L. Slomberg and M. H. Schoenfisch, *J. Biomed. Mater. Res., Part A*. **2014**, *103 (6), 1974-1984*.

[171] A. W. Carpenter, B. V. Worley, D. L. Slomberg and M. H. Schoenfisch, *Biomacromolecules*, **2012**, *13*, 3334– 3342.

[172] L. J. Taite, P. Yang, H.-W. Jun and J. L. West, *J. Biomed. Mater. Res., Part B*, **2007**, *84*, 108–116.

[173] Q. Liu, P. Singha, H. Handa, J. Locklin, *Langmuir* **2017**, *33(45)*, 13105–13113.

[174] T-K. Nguyen, R. Selvanayagam, K. K. K. Ho, R. Chen, S. K. Kutty, S. A. Rice, N. Kumar, N. Barraud, H. T. T. Duong, C. Boyer, *Chem. Sci*., **2016**, *7*, 1016-1027.

[175] P. G. Wang, M. Xian, X. Tang, X. Wu, Z. Wen, T. Cai and A. J. Janczuk, *Chem. Rev.*, **2002**, *102*, 1091–1134.

Author Manuscript

This article is protected by copyright. All rights reserved

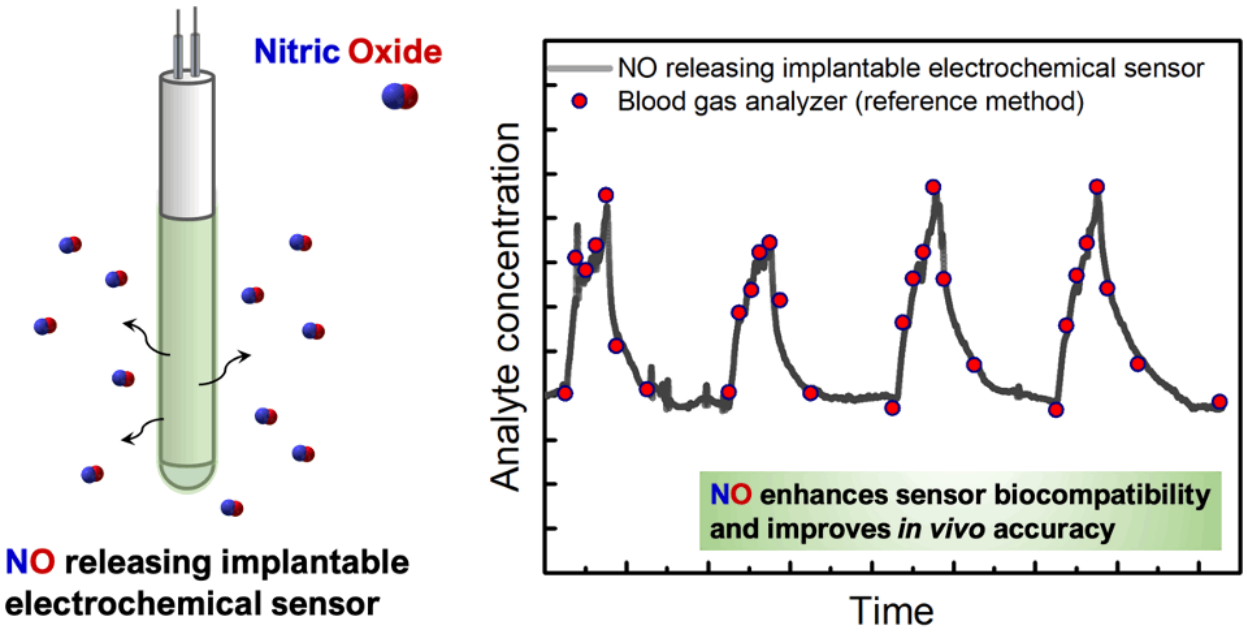

Table of Contents (TOC)

Author Manuscript

This article is protected by copyright. All rights reserved

Table and figure captions

Table 1. Summary of NO releasing electrochemical sensors reported to date.

Fig. 1. Illustration of (a) thrombus formation processes on the surface of an implanted intravascular chemical sensor and (b) the corresponding typical sensor signal drift associated with progressive thrombus formation for the different types of intravascular chemical sensors.

Fig. 2. Schematic representation of three major NO-release strategies used for fabricating NO-releasing implantable chemical sensors including: (a) coating of N-diazeniumdiolates or RSNO species doped polymer to sensor surface; (b) *in situ* NO generation from endogenous RSNOs using catalysts (Cu(II)-complexes, organoseleniums, etc.) doped polymer coating; and (c) electrochemically modulated NO generation from inorganic nitrite.

Fig. 3. (a) Cross-sectional schematic view of dual-lumen catheter-type amperometric NO generating/releasing PO_2 sensor; b) degree of thrombus coverage of control and NO release oxygen sensing dual lumen catheters after implantation in sheep veins/arteries for 18 h; (c) the comparison of relative deviation in measuring oxygen levels in blood using electrochemical NO releasing sensors (black square) and a control sensors (NO release not turned on) (red square) implanted in pig arteries for 19 h benchmarked to *in vitro* test values (blue line). (Adapted from [130] with permission; copyright 2015, the American Chemical Society).

Fig. 4. Image and cross-sectional schematic view of a dual-lumen catheter-type potentiometric NO-releasing PCO_2 sensor. (Adapted from [133] with permission; copyright 2020, the American Chemical Society).

Fig. 5. (a) Example of response curves for a dual-lumen catheter-type potentiometric NO-releasing PCO_2 sensor (green) and a control sensor (blue) for PCO_2 monitoring in pig femoral arteries compared to corresponding discrete blood gas analyzer values (red dots) over a 20-h animal study; (b) images of NO releasing and control sensors explanted from pig femoral arteries after 20 h; (c) Comparison of PCO_2 values measured by NO releasing arterial PCO_2 ($PaCO_2$) sensors and venous PCO_2 ($PvCO_2$) sensors (left) and control sensors (right) against the values by a blood gas analyzer throughout the 20-h animal studies. The dashed lines and the solid lines indicate 0% error and ± 20% error. (Adapted from [133] with permission; copyright 2020, the American Chemical Society).

Fig. 6. (a) Schematic of needle-type NO-releasing electrochemical glucose biosensor, modified to store NO by doping NO-releasing silica nanoparticles into the outermost, glucose flux-limiting polyurethane layer; (b) Comparison of MARD for the sensors measured percutaneously using a diabetic swine model, with 14 d (red)

Author Manuscript

This article is protected by copyright. All rights reserved

and 30 d (black) NO-releasing (solid) vs. the corresponding control (dashed) sensor membranes. Statistical significance from control at a given time point is denoted by asterisks (*$p < 0.05$; **$p < 0.01$). (Reproduced from [145] with permission; copyright 2019, the American Chemical Society).

Fig. 7. (a) NO-releasing needle/catheter type glucose sensor design with DBHD/N_2O_2 as the NO donor; (b) images of the control (top) and NO release (bottom) glucose sensors after 7 h of *in vivo* experiment in rabbit veins. The portion to the left of the dashed lines were inside of the veins; (c) comparison of glucose concentration values obtained from benchtop blood gas analyzer and the converted current values measured by the continuous sensor. The conversion of current to glucose concentration ($mmol^{-1}$) was made either with the calibration curve in bovine serum or a one-point calibration. (Adapted from [147] with permission; copyright 2015, Elsevier).

Author Manuscript

This article is protected by copyright. All rights reserved

Table 1. Summary of NO releasing electrochemical sensors reported to date.

Analyte	NO Releasing Materials/Methods	Study Method	Sensor Performance	Year	Ref
H^+, K^+	DMHD/N_2O_2	*In vitro*	The first NO releasing electrochemical (ion) sensors. No interference from NO to sensor performance. *In vitro* study in sheep plasma showed inhibited platelet adhesion.	1997	[66]
H^+, K^+, PO_2	MAHMA/N_2O_2 LPEI/N_2O_2 mompipPVC/N_2O_2	*In vitro*	The first NO releasing Clark-style amperometric oxygen sensors. Three distinctly different types of diazeniumdiolate NO donors were developed to release NO for > 48 h.	1999	[124]
PO_2	MAHMA/N_2O_2	Dog model, intravascular	The first *in vivo* study to demonstrate reduced clot-formation and improved *in vivo* (intra-arterial) accuracy of an NO releasing IV sensor.	2000	[125]
PO_2	DACA-6/N_2O_2	Porcine model, intravascular	NO donors were covalently linked to the silicone polymer coating alleviated leaching and potential nitrosamine toxicity of diazeniumdiolates; minimal sensing deviation was observed from NO releasing sensor while the control had a -28% average deviation (after 15 h).	2002	[126]
PO_2	Sol-gel diazeniumdiolate	*In vitro*	Sol–gel derived diazeniumdiolate materials were used as NO donors in amperometric oxygen sensors.	2004	[127]
Glucose	MTMOS diazeniumdiolate	*In vitro*	A hybrid NO donor modified sol-gel particle-doped polyurethane was used for amperometric glucose sensor fabrication.	2004	[138]
Glucose	MTMOS diazeniumdiolate	*In vitro*	Micropatterned NO-releasing xerogel lines were formed on top of glucose sensor to provide NO-release (48 h) to minimize disruption of sensor performance by top NO releasing coating.	2005	[139]
Glucose	DBHD/N_2O_2	Rat model, subcutaneous	The first *in vivo* glucose sensors. DBHD/N_2O_2 was used to release NO. Clarke error grid revealed enhanced accuracy for NO releasing sensors over 3 d, and inflammatory response was significantly decreased for 100% at 24 h.	2005	[137]
Glucose	Xerogel diazeniumdiolate	Buffer	PVP was doped into GOx-containing NO-releasing xerogel to improve glucose sensor sensitivity. Leaching of enzymes exists	2006	[140]
PO_2	Endogenous GNSO	Porcine model, intravascular	The first study to dope Cu^0 particles into the outermost PU membrane of PO_2 sensor to catalytically convert endogenous *S*-nitrosothiols in blood to NO. 20 h of *in vivo* experiment in porcine arteries showed significantly inhibited thrombus formation and enhanced oxygen sensing accuracy via NO release.	2007	[128]
Glucose, Lactate	DBHD/N_2O_2	Rabbit model, intravascular	Glucose sensors were for the first time tested (for 7 h) intravascularly in rabbit veins. Clark error grid analysis shows that the NO releasing sensors had 97.5% of data points in Zone A and B while the value was 86.7% for the controls. Lactate sensors with a similar design were also proposed.	2011	[146]
Glucose	NO donor-modified (PAMAM G4-ED) dendrimers	*In vitro*	An NO-releasing porous electrospun fiber mat was used for glucose sensor design.	2011	[142]
Glucose	NO donor-modified diazeniumdiolate and RSNO silica vehicles	*In vitro*	NO fluxes and delivery totals as well as the glucose sensor characteristics (e.g., response time, sensitivity and dynamic range) were proven to be tunable with different NO donating systems.	2013	[141]
Glucose	MAP3/NO and MPTMS-RSNO	Porcine model, percutaneous	Performances of NO-releasing glucose sensors with both short-term (MAP3/NO based) and long-term (MPTMS-RSNO based) releasing profiles were compared *in vivo*.	2014	[143]
Glucose	DBHD/N_2O_2	Rabbit model, intravascular	E2As was selected as a replacement for the PurSil for better biocompatibility in IV glucose sensors.	2015	[147]
PO_2	Catalyzed electrochemical reduction of nitrite ions	Rabbit and Porcine, intravascular	Electrochemical reduction of nitrite ions was for the first time implemented in electrochemical sensor design. Hemocompatibility and *in vivo* accuracy were both significantly improved in both rabbit (7 h) and porcine (20 h).	2015	[130]

Author Manuscript

This article is protected by copyright. All rights reserved

Glucose	SNAP	Buffer *In vitro*	The first 2nd-generation NO releasing glucose sensor design.	2017	[148]
Glucose	MPTMS-RSNO	*In vitro*	Glucose sensor analytical performance, NO-release kinetics and donor leaching from the sensor membranes were evaluated as a function of NO-releasing particle and polyurethane (PU) chemistries.	2017	[144]
Lactate	SNAP	Porcine, intravascular & subcutaneous	Preliminary results of IV continuous blood lactate measurements using NO-releasing amperometric enzyme sensors were presented, though the animals were under systemic heparinization.	2018	[153]
PO_2	SNAP	Rabbit and porcine, intravascular	Clark-type IV PO_2 sensors with a SNAP-impregnated catheters configuration provided notable improvement on thrombus formation and analytical *in vivo* sensing performance.	2019	[129]
Glucose	MPTMS-RSNO	Diabetic porcine, percutaneous	NO release from subcutaneous glucose sensors directly corresponded with improved numerical and clinical accuracy and reduced FBR-associated inflammatory biomarkers in diabetic swine. Sensors doped with porous NO-releasing particles were capable of 30 d of active release in animal, maintained standard-compliant accuracy for >3 weeks.	2019	[145]
PCO_2	SNAP	Porcine model, intravascular	The first NO releasing dual-lumen potentiometric carbon dioxide sensor with much improved IV accuracy and hemocompatibility for 20 h.	2020	[133]

Author Manuscript

This article is protected by copyright. All rights reserved

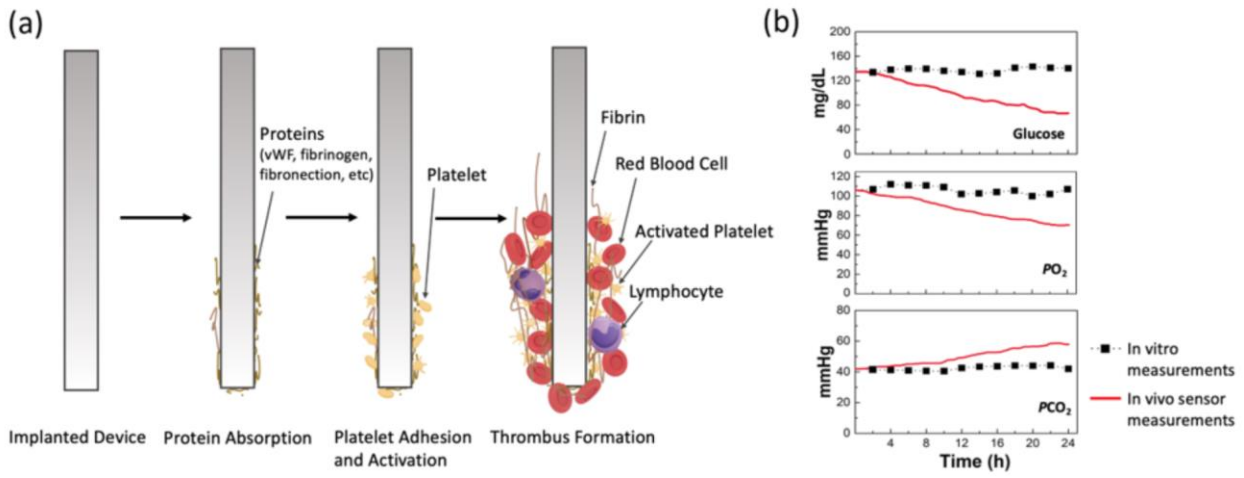

Fig. 1. Illustration of (a) thrombus formation processes on the surface of an implanted intravascular chemical sensor and (b) the corresponding typical sensor signal drift associated with progressive thrombus formation for the different types of intravascular chemical sensors.

Author Manuscript

This article is protected by copyright. All rights reserved

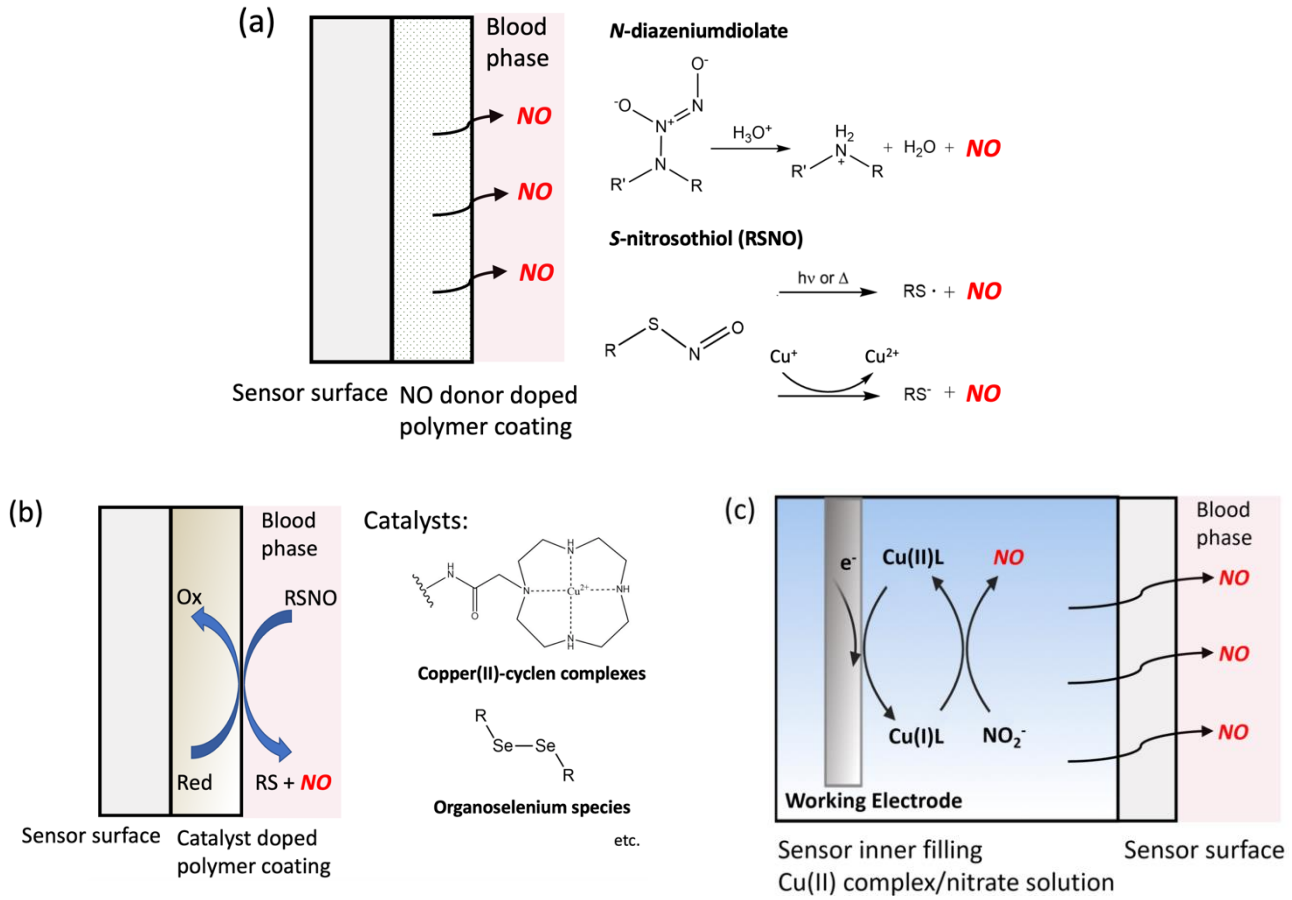

Fig. 2. Schematic representation of three major NO-release strategies used for fabricating NO-releasing implantable chemical sensors including: (a) coating of N-diazeniumdiolates or RSNO species doped polymer to sensor surface; (b) *in situ* NO generation from endogenous RSNOs using catalysts (Cu(II)-complexes, organoseleniums, etc.) doped polymer coating; and (c) electrochemically modulated NO generation from inorganic nitrite.

This article is protected by copyright. All rights reserved

Author Manuscript

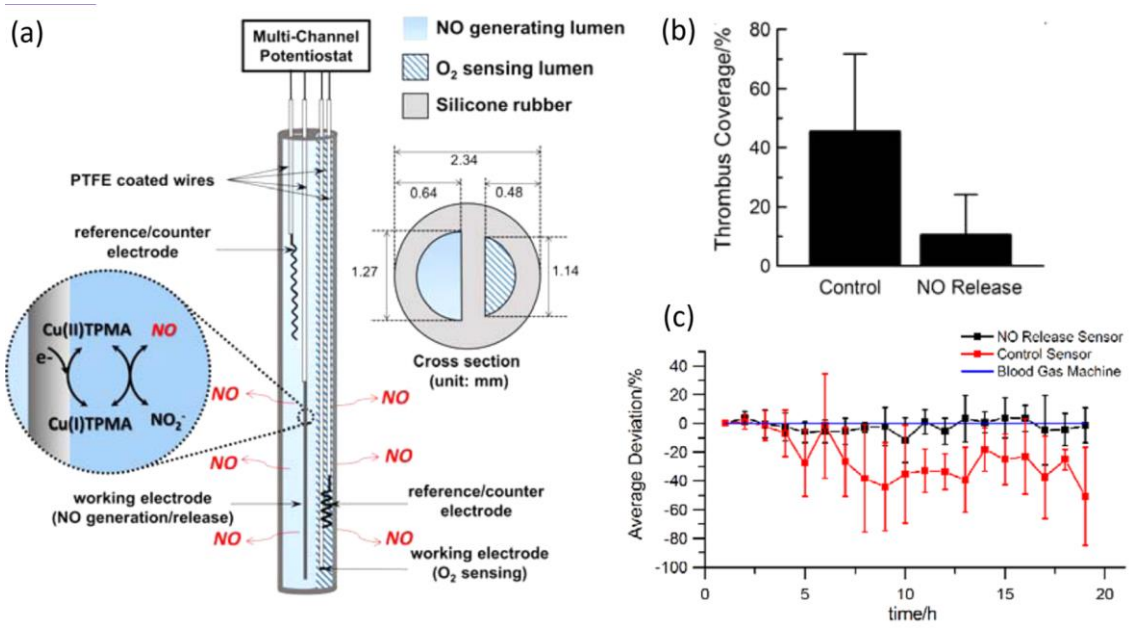

Fig. 3. (a) Cross-sectional schematic view of dual-lumen catheter-type amperometric NO generating/releasing PO_2 sensor; b) degree of thrombus coverage of control and NO release oxygen sensing dual lumen catheters after implantation in sheep veins/arteries for 18 h; (c) the comparison of relative deviation in measuring oxygen levels in blood using electrochemical NO releasing sensors (black square) and a control sensors (NO release not turned on) (red square) implanted in pig arteries for 19 h benchmarked to *in vitro* test values (blue line). (Adapted from [130] with permission; copyright 2015, the American Chemical Society).

Author Manuscript

This article is protected by copyright. All rights reserved

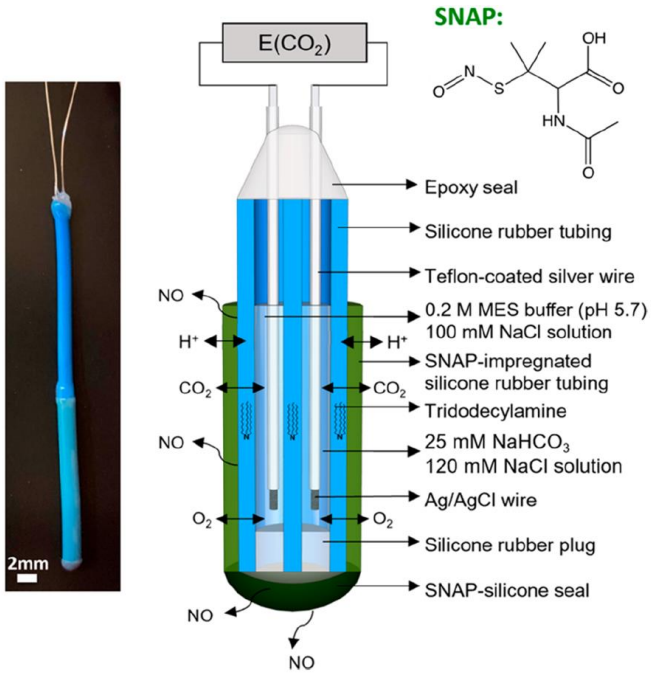

Fig. 4. Image and cross-sectional schematic view of a dual-lumen catheter-type potentiometric NO-releasing *P*CO_2 sensor. (Adapted from [133] with permission; copyright 2020, the American Chemical Society).

Author Manuscript

This article is protected by copyright. All rights reserved

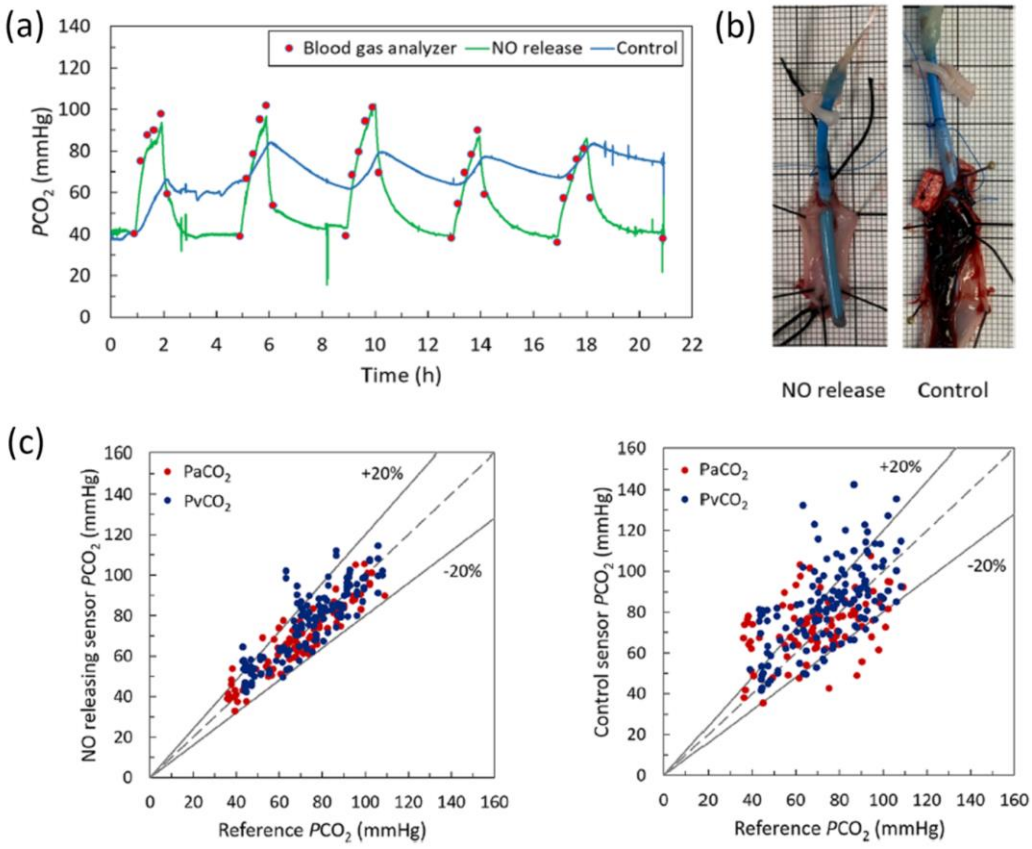

Fig. 5. (a) Example of response curves for a dual-lumen catheter-type potentiometric NO-releasing PCO_2 sensor (green) and a control sensor (blue) for PCO_2 monitoring in pig femoral arteries compared to corresponding discrete blood gas analyzer values (red dots) over a 20-h animal study; (b) images of NO releasing and control sensors explanted from pig femoral arteries after 20 h; (c) Comparison of PCO_2 values measured by NO releasing arterial PCO_2 ($PaCO_2$) sensors and venous PCO_2 ($PvCO_2$) sensors (left) and control sensors (right) against the values by a blood gas analyzer throughout the 20-h animal studies. The dashed lines and the solid lines indicate 0% error and ± 20% error. (Adapted from [133] with permission; copyright 2020, the American Chemical Society).

Author Manuscript

This article is protected by copyright. All rights reserved

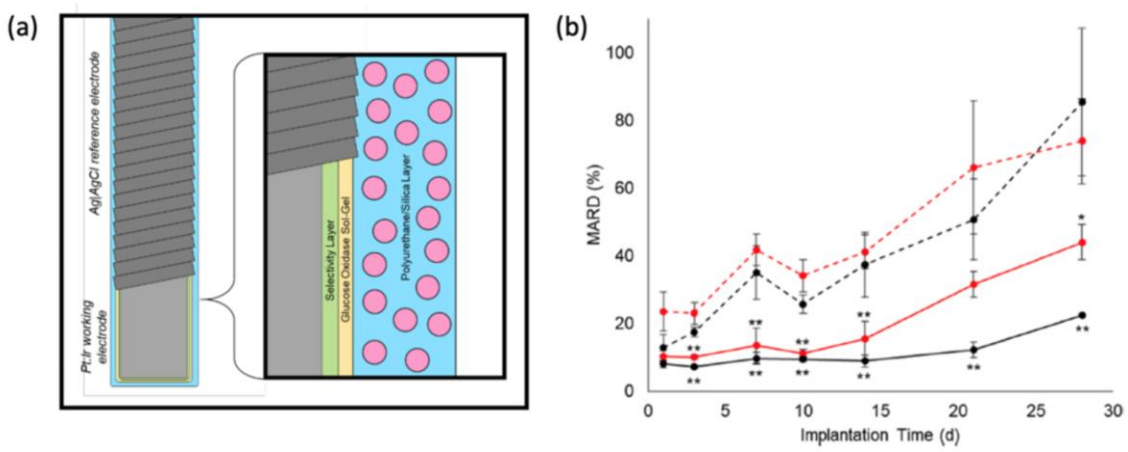

Fig. 6. (a) Schematic of needle-type NO-releasing electrochemical glucose biosensor, modified to store NO by doping NO-releasing silica nanoparticles into the outermost, glucose flux-limiting polyurethane layer; (b) Comparison of MARD for the sensors measured percutaneously using a diabetic swine model, with 14 d (red) and 30 d (black) NO-releasing (solid) vs. the corresponding control (dashed) sensor membranes. Statistical significance from control at a given time point is denoted by asterisks (*$p < 0.05$; **$p < 0.01$). (Reproduced from [145] with permission; copyright 2019, the American Chemical Society).

Author Manuscript

This article is protected by copyright. All rights reserved

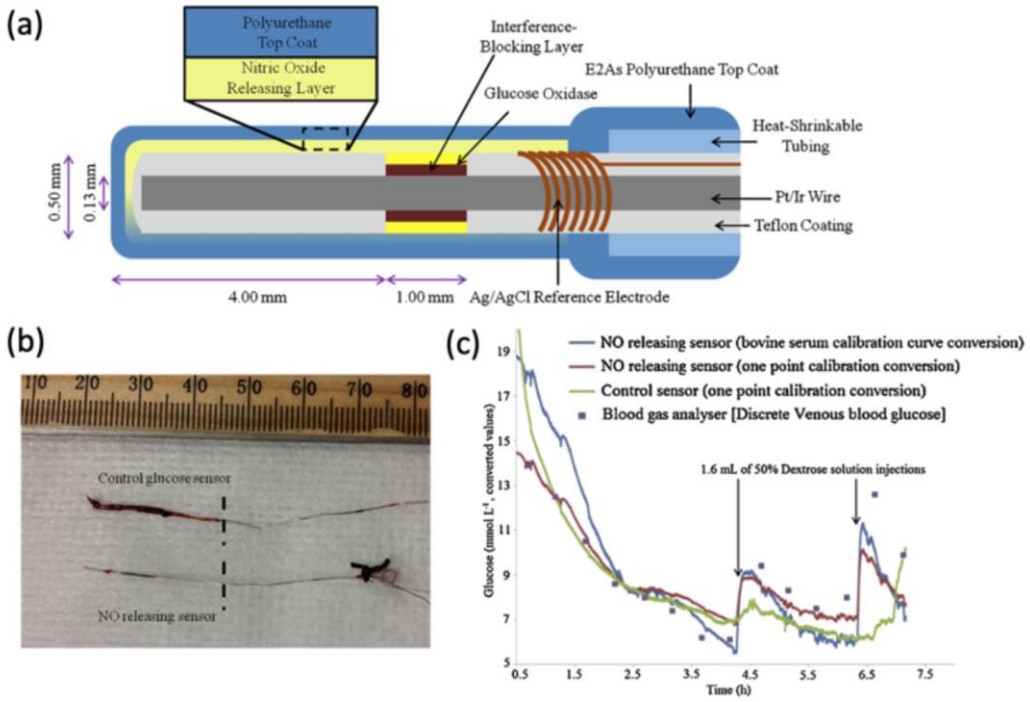

Fig. 7. (a) NO-releasing needle/catheter type glucose sensor design with DBHD/N_2O_2 as the NO donor; (b) images of the control (top) and NO release (bottom) glucose sensors after 7 h of *in vivo* experiment in rabbit veins. The portion to the left of the dashed lines were inside of the veins; (c) comparison of glucose concentration values obtained from benchtop blood gas analyzer and the converted current values measured by the continuous sensor. The conversion of current to glucose concentration ($mmol^{-1}$) was made either with the calibration curve in bovine serum or a one-point calibration. (Adapted from [147] with permission; copyright 2015, Elsevier).

This article is protected by copyright. All rights reserved

Author Manuscript